Deep Learning Based Processing of EEG Signals for Detection and Recognition of Parkinson Disease

Samed Reyhanlı

Submitted to the
Institute of Graduate Studies and Research
in partial fulfillment of the requirements for the degree of

Master of Science
in
Computer Engineering

Eastern Mediterranean University
August 2022
Gazimağusa, North Cyprus

Approval of the Institute of Graduate Studies and Research

Prof. Dr. Ali Hakan Ulusoy
Director

I certify that this thesis satisfies all the requirements as a thesis for the degree of Master of Science in Computer Engineering.

Prof. Dr. Hadi Işık Aybay
Chair, Department of Computer Engineering

We certify that we have read this thesis and that in our opinion it is fully adequate in scope and quality as a thesis for the degree of Master of Science in Computer Engineering.

Assoc. Prof. Dr. Adnan Acan
Supervisor

Examining Committee

1. Assoc. Prof. Dr. Adnan Acan

2. Asst. Prof. Dr. Mehtap Köse Ulukök

3. Asst. Prof. Dr. Ahmet Ünveren

ABSTRACT

The aim of this study is to provide early detection of Parkinson's disease by processing EEG signals through two dimensional colored image transforms.

Parkinson's disease is a neurological disease that usually occurs in old ages and occurs with a decrease in dopamine levels in the brain. There is no known treatment for Parkinson's disease. Early detection and early treatment in Parkinson's disease is very important to slow the progression of the disease.

EEG data were obtained from the UC San Diego Resting State EEG Database from Patients with Parkinson's disease. EEG signals were converted to GASF images by going through various preprocessing steps.

AlexNet deep learning model was used to train and test the obtained 2D colored image data. AlexNet is a Convolutional Neural Network model consisting of 8 layers. In the literature review, 16 channels used in various studies were selected. Amoung these Fp1, F7 and F3 channels are the ones with highest reported succes results. The same channels are also considered with in the scope of address in this thesis work.

GASF images of selected Fp1, F7 and F3 channels were used to train the AlexNet CNN model over 100 epochs. The developed model achieved promising performance with 97.72% accuracy, 97.76% sensitivity and 97.68% specificity. In addition, the AlexNet CNN model was trained and tested over 100 epochs with 4-fold Cross Validation.

As a result of this study, the developed model achieved the highest results with 97.73% accuracy, 97.94% sensitivity and 97.53% specificity.

Keywords: parkinson disease, deep learning, eeg, gasf, cnn.

ÖZ

Bu çalışmanın amacı, iki boyutlu renkli görüntü dönüşümlerini işleyerek Parkinson hastalığının erken tespitini sağlamaktır.

Parkinson hastalığı, genellikle ileri yaşlarda ortaya çıkan ve beyindeki dopamin seviyesinin düşmesiyle ortaya çıkan nörolojik bir hastalıktır. Parkinson hastalığının bilinen bir tedavisi yoktur. Parkinson hastalığında erken teşhis ve erken tedavi, hastalığın ilerlemesini yavaşlatmak için çok önemlidir.

EEG verileri, Parkinson hastalığı olan Hastalardan alınan UC San Diego Dinlenme Durumu EEG Veritabanından elde edilmiştir. EEG sinyalleri çeşitli ön işleme adımlarından geçirilerek GASF görüntülerine dönüştürülmüştür.

Elde edilen verileri eğitmek ve test etmek için AlexNet derin öğrenme modeli kullanıldı. AlexNet, 8 katmandan oluşan bir Evrişimsel Sinir Ağı modelidir. Literatür taramasında çeşitli çalışmalarda kullanılan 16 kanal seçilmiş ve bu kanallar arasından en yüksek sonucu veren Fp1, F7 ve F3 kanalları nihai sonuç için kullanılmıştır. Bu seçim yapılırken her kanal ayrı ayrı eğitilmiş ve test edilmiştir. Elde edilen sonuçlar analiz edilirken doğruluğu en yüksek olan kanallar seçilmiştir.

Seçilen Fp1, F7 ve F3 kanallarının GASF görüntüleri AlexNet CNN modelinde 100 dönem boyunca eğitilmiştir. Geliştirilen model %97,72 doğruluk, %97,76 duyarlılık ve %97,68 özgüllük ile umut verici bir performans elde etmiştir. Ayrıca, AlexNet CNN modeli, k-Fold Cross Validation kullanılarak 4-fold ile 100 epoch boyunca eğitilmiş

ve test edilmiştir. 4-Fold sonucunda geliştirilen model %97.73 doğruluk, %97.94 duyarlılık ve %97.53 özgüllük ile en yüksek sonuçlar elde edilmiştir.

Keywords: parkinson hastalığı, derin öğrenme, eeg, gasf, cnn.

DEDICATION

To my family

ACKNOWLEDGMENT

I would like to record my gratitude to Assoc. Prof. Dr. Adnan ACAN for his supervision, advice, and guidance from the very early stage of this thesis as well as giving me extraordinary experiences throughout the work. Above all and the most needed, he provided me constant encouragement and support in various ways. His ideas, experiences, and passions has truly inspire and enrich my growth as a student. I am indebted to him more than he knows.

TABLE OF CONTENTS

ABSTRACT iii

ÖZ v

DEDICATION vii

ACKNOWLEDGMENT viii

LIST OF TABLES xi

LIST OF FIGURES xii

LIST OF ABBREVIATIONS xii

1 INTRODUCTION 1

1.1 Parkinson's Disease 1

1.1.1 Diagnostic Methods of Parkinson's Disease 4

1.1.2 Treatment in Parkinson's Disease 5

1.2 Literature Review 5

2 ELECTROENCEPHALOGRAPHY 12

3 CONVOLUTIONAL NEURAL NETWORKS 18

4 GRAMIAN ANGULAR FIELD IMAGES 22

5 K-FOLD CROSS VALIDATION 26

6 METHODOLOGY 28

6.1 Participants 30

6.2 Data Collection 30

6.3 Data Preprocessing 32

7 RESULTS AND DISCUSSIONS 41

7.1 Preparation of the Working Environment 41

7.1.1 EEG Channel Fp1 43

7.1.2 EEG Channel F7 45
7.1.3 EEG Channel F3 47
7.1.4 EEG Channel C3 49
7.1.5 EEG Channel P3 51
7.1.6 EEG Channel Pz 53
7.1.7 EEG Channel O1 55
7.1.8 EEG Channel Oz 57
7.1.9 EEG Channel O2 59
7.1.10 EEG Channel P4 61
7.1.11 EEG Channel C4 63
7.1.12 EEG Channel F4 65
7.1.13 EEG Channel F8 67
7.1.14 EEG Channel Fp2 69
7.1.15 EEG Channel Fz 71
7.1.16 EEG Channel Cz 73
7.2 General Results 75
7.2.1 General Results With K-Fold 79
7.3 Discussion 81
8 CONCLUSION 83
9 IN THE FUTURE 84
REFERENCES 85

LIST OF TABLES

Table 1: EEG test different frequency ranges 16

Table 2: Results of all channels.....75

Table 3: Another studies with dataset and channels.....81

Table 4: Results and other studies 82

LIST OF FIGURES

Figure 1: A file structure of the BIDS standard [1] 7

Figure 2: EEG – Cap [7] 14

Figure 3: EEG simple electrode layouts[8] 15

Figure 4: EEG Detailed electrode layouts[9] 15

Figure 5: AlexNet Architecture [11].....19

Figure 6: Tanh, ReLU, Sigmoid, Linear coordinate plane [13] 20

Figure 7: AlexNet's layers and number of parameters.....21

Figure 8: GASF-GADF compared with 9 different methods.....25

Figure 9: K-fold cross validation working logic [15] 27

Figure 10: BIDS standard.....29

Figure 11: Channels available in the dataset used 31

Figure 12: Headplot view with LetsWave7 HC 32

Figure 13: Topograph view with LetsWave7 HC 32

Figure 14: Headplot view with LetsWave7 PD-OFF 32

Figure 15: Topograph view with LetsWave7 PD-OFF.....33

Figure 16: Headplot view with LetsWave7 PD-ON.....33

Figure 17: Topograph view with LetsWave7 PD-ON 33

Figure 18: EEG recording of the HC-4 participant 34

Figure 19: HC4 - filtered from 0-1 range of participant 35

Figure 20: HC4 - filtered from 94-96 range of participant 35

Figure 21: The O1 channel data of the HC4 participant 36

Figure 22: Figure 20: HC4 - filtered from 0-5 range of participant 37

Figure 23: O1 channel results of HC4 participant.....38

Figure 24: Selected channels for train and test.....42
Figure 25: Fp1 channel HC and PD-ON Confusion Matrix 43
Figure 26: Fp1 channel HC and PD-OFF Confusion Matrix.....44
Figure 27: F7 channel HC and PD-ON Confusion Matrix 45
Figure 28: F7 channel HC and PD-OFF Confusion Matrix.....46
Figure 29: F3 channel HC and PD-ON Confusion Matrix 47
Figure 30: F3 channel HC and PD-OFF Confusion Matrix.....48
Figure 31: C3 channel HC and PD-ON Confusion Matrix.....49
Figure 32: C3 channel HC and PD-OFF Confusion Matrix 50
Figure 33: P3 channel HC and PD-ON Confusion Matrix 51
Figure 34: P3 channel HC and PD-OFF Confusion Matrix.....52
Figure 35: Pz channel HC and PD-ON Confusion Matrix.....53
Figure 36: Pz channel HC and PD-OFF Confusion Matrix 54
Figure 37: O1 channel HC and PD-ON Confusion Matrix.....55
Figure 38: O1 channel HC and PD-OFF Confusion Matrix 56
Figure 39: Oz channel HC and PD-ON Confusion Matrix.....57
Figure 40: Oz channel HC and PD-OFF Confusion Matrix 58
Figure 41: O2 channel HC and PD-ON Confusion Matrix.....59
Figure 42: O2 channel HC and PD-OFF Confusion Matrix 60
Figure 43: P4 channel HC and PD-ON Confusion Matrix 61
Figure 44: P4 channel HC and PD-OFF Confusion Matrix.....62
Figure 45: C4 channel HC and PD-ON Confusion Matrix.....63
Figure 46: C4 channel HC and PD-OFF Confusion Matrix 64
Figure 47: F4 channel HC and PD-ON Confusion Matrix 65
Figure 48: F4 channel HC and PD-OFF Confusion Matrix.....66

Figure 49: F8 channel HC and PD-ON Confusion Matrix 67
Figure 50: F8 channel HC and PD-OFF Confusion Matrix.....68
Figure 51: Fp2 channel HC and PD-ON Confusion Matrix 69
Figure 52: Fp2 channel HC and PD-OFF Confusion Matrix.....70
Figure 53: Fz channel HC and PD-ON Confusion Matrix.....71
Figure 54: Fz channel HC and PD-OFF Confusion Matrix 72
Figure 55: Cz channel HC and PD-ON Confusion Matrix 73
Figure 56: Cz channel HC and PD-OFF Confusion Matrix.....74
Figure 57: Fp1, F7, F3 channel HC and PD-OFF Confusion Matrix 77
Figure 58: Fp1, F7, F3 channel HC and PD-ON Confusion Matrix.....78
Figure 59: Fp1, F7, F3 channel HC and PD-OFF Confusion Matrix 79
Figure 60: Fp1, F7, F3 channel HC and PD-ON Confusion Matrix.....80

LIST OF ABBREVIATIONS

ANN	Artificial Neural Network
CNN	Convolutional Neural Network
EEG	Electroencephalogram
GADF	Gramian Difference Angular Field
GAF	Gramian Angular Field
GASF	Gramian Summation Angular Field
HC	Health Control
LSSVM	Least Squares Support Vector Machine Classifiers
PD	Parkinson's Disease
RNN	Recurrent Neural Network

Chapter 1

INTRODUCTION

1.1 Parkinson's Disease

Parkinson's disease was first described in the literature in 1817 by James Parkinson, an English surgeon and pharmacist, with the name shaky palsy. Later, it was named as Parkinson's disease in the literature by Jean Martin Charcot. Parkinson's disease is a neurological disease that progresses over time. Thanks to the dopamine hormone secreted in the human brain, smooth and coordinated movements of the body are ensured. Dopamine is secreted in a part of the brain called the Substantia-Nigra. In people with Parkinson's disease, cells in the Substantia-Nigra area begin to die and not enough dopamine can be secreted in the body. It is not known exactly what causes this. As the dopamine level in the body drops, Parkinson's disease begins to appear. Parkinson's disease, which presents with mild tremors, stiffness in the arms, stiffness in the fingers, and slowed down movements, is defined as a type of disease that, if left untreated, can increase the symptoms over time and make the patient bedridden.

Parkinson's disease generally occurs in old age. The disease is most common between the ages of 40 and 75. People over the age of 65 have the highest risk of developing Parkinson's disease. The incidence of the disease above the age of 65 is 1%. 1 out of every 100 people over the age of 65 has Parkinson's disease. However, contrary to what is known, Parkinson's disease can occur not only at older ages, but also at younger ages. Even if it is not very common, 5% of individuals with Parkinson's disease are

young individuals between the ages of 20-40. Parkinson's disease is more common in men than women. Considering the data collected so far, it has been concluded that Parkinson's disease is seen 50% more in men compared to women.

Symptoms of Parkinson's disease are not observed suddenly in the patient and are not severe at first. Parkinson's disease has been defined as a slowly progressive neurological disease. There are 4 main symptoms of Parkinson's disease. These are; tremors that occur at rest, muscle stiffness, posture disorder and slowing of movements. The patient loses his mobility a little at first. While speaking, the person cannot use his facial expressions as before and starts to speak with fixed facial expressions.

Since the disease is usually seen over the age of 65, the people around the patient do not see this as a sign of a disease. This situation can only be noticed by the relatives of the patient. Other symptoms of Parkinson's disease include slurred speech, stiffness in the legs, trembling in the fingers, and drooling. Symptoms usually start on only one side of the body and over time appear on the other side as well. As the symptoms are first seen on only one side of the body, one leg may be observed to move more slowly while walking. Depending on which region the disease affects, the treatment to be applied or the course of the disease may also vary. Even in the early stages of the disease, the patient may find difficulties in swallowing. In this process, the patient begins to speak with a lower voice. However, if the disease started in the lower part of the body, this process will show symptoms in the feet and legs. Parkinson's is a genetic disease. However, having Parkinson's disease in the family does not always mean that this disease can be caught. Environmental factors are as important as genetics.

Parkinson's disease progresses in stages. Parkinson's disease has 5 stages in total. In the early stages of the disease, damage to the brain is minimal. With each progressive stage, the damage to the brain increases. As a result, the patient's quality of life decreases.

Phase 1 :

The disease usually affects only one side of the body. For example, it may manifest itself as a loss of movement and minor tremors in the fingers of only one hand. The patient's facial expression becomes monotonous and mimic loss occurs. Symptoms are usually not very noticeable. These symptoms cannot be easily understood by an individual looking from the outside. However, it can be noticed by the relatives of the patient.

Phase 2 :

Parkinson's patients go into the second stage 3-4 years after they get the disease. The disease now affects both sides of the body. Visible tremors and movement disorders occur in the body. At this stage, disorders in the posture of the sick individuals began to occur. Gait disturbances can now be easily noticed by anyone. The disease does not directly affect the person's normal life. The patient continues his life with these symptoms.

Phase 3 :

At this stage, the damage to the brain has progressed. The patient's hand movements and gait are slowed down. The patient has difficultt in walking. He may lose his balance and fall while walking. This stage is the middle stage of the disease. Moderate dysfunction is observed in patients.

Phase 4 :

In this stage, the damage to the brain is intensified. All symptoms become severe. The patient has difficulty in standing up and has become unable to walk. Although all symptoms increase at this stage, a decrease in the patient's tremor can be observed. The patient can move, albeit with difficulty. However, these movements are limited and very slow. At this stage, patients can no longer sustain their lives on their own and need help.

Phase 5 :

Stage 5 is the final stage of the disease. The damage to the brain has reached the highest level. All of the patient's mobility is lost. At this stage, the patient cannot get out of bed and becomes bedridden. At this stage, the patient becomes completely dependent on care.

1.1.1 Diagnostic Methods of Parkinson's Disease

Parkinson's disease can be diagnosed by a physician. The medical history of the patient is reviewed by the doctor and a physical examination is performed. There is no specific test or measurement used to diagnose Parkinson's disease. Various tests are performed to establish the diagnosis. However, none of these tests alone is sufficient to make a diagnosis. While making the diagnosis, MRI, blood tests, lumbar puncture or radiological imaging methods are used. There is no stable method among these methods. Diagnosis of the disease is generally made by examining the patient's medical history and physical examination. An early and accurate diagnosis is very important. Thanks to a diagnosis made when the disease is in the 1st stage, treatment can start early and supplements can be taken before the damage to the brain grows.

Thanks to early diagnosis, the progression of the stages of the disease can be slowed down.

1.1.2 Treatment in Parkinson's Disease

There is no treatment method that will cure Parkinson's disease or stop its progression completely. If the diagnosis of Parkinson's is made correctly and early, the patient can respond very well to the treatment. With an early and accurate diagnosis, it is possible to get treatment results above 90%. Treatment is divided into drug therapy and surgical treatment. After the diagnosis of Parkinson's disease, drugs are used to eliminate dopamine deficiency in the brain. Treatment is started with oral medications in the early stages of the disease. Parkinson's disease drugs with the active ingredient levodopa are the most commonly used drugs in the early stages. The progression of disease stages can be slowed down by regular use of medication. As the disease progresses, oral medications may be insufficient. In this case, some surgical treatment methods such as apomorphine injections or injecting the drug directly into the intestine can be applied. However, these methods are only used when oral medications are not sufficient. Surgery may be used for Parkinson's disease. However, this may only be beneficial in suitable patients. Surgical methods known as ablation and brain battery may not be suitable for every patient. As a result, no drug treatment or surgical intervention is sufficient to completely eliminate the disease. With these treatments, only the progression of the disease can be slowed down.

1.2 Literature Review

In this section, a literature review on deep learning approaches for Methods of Displaying Time Series to Improve Classification, electroencephalogram analysis based on gramian angular field transformation. However, if the disease started in the lower part of the body, this process will show symptoms in the feet and legs. However,

if the disease started in the lower part of the body, this process will show symptoms in the feet and legs. However, if the disease started in the lower part of the body, this process will show symptoms in the feet and legs However, if the disease started in the lower part of the body, this process will show symptoms in the feet and legs. In addition, these sub-areas are briefly mentioned.

Pernet et al. developed and standart to enable researchers to easily organize and share brain data [1].

The name of this standard (BIDS) is The Brain Imaging Data Structure project. In this standard, unlike other standards, some general tools and references for EEG data are presented. The BIDS EEG dataset extension closely follows the general BIDS specification. Each patient’s or subject's data is stored in subdirectories. At the top of the file structure there is a json file that gives general information about the dataset. This file, named as dataset-description and called eeg.json, provides comprehensive general information about the EEG registration system.

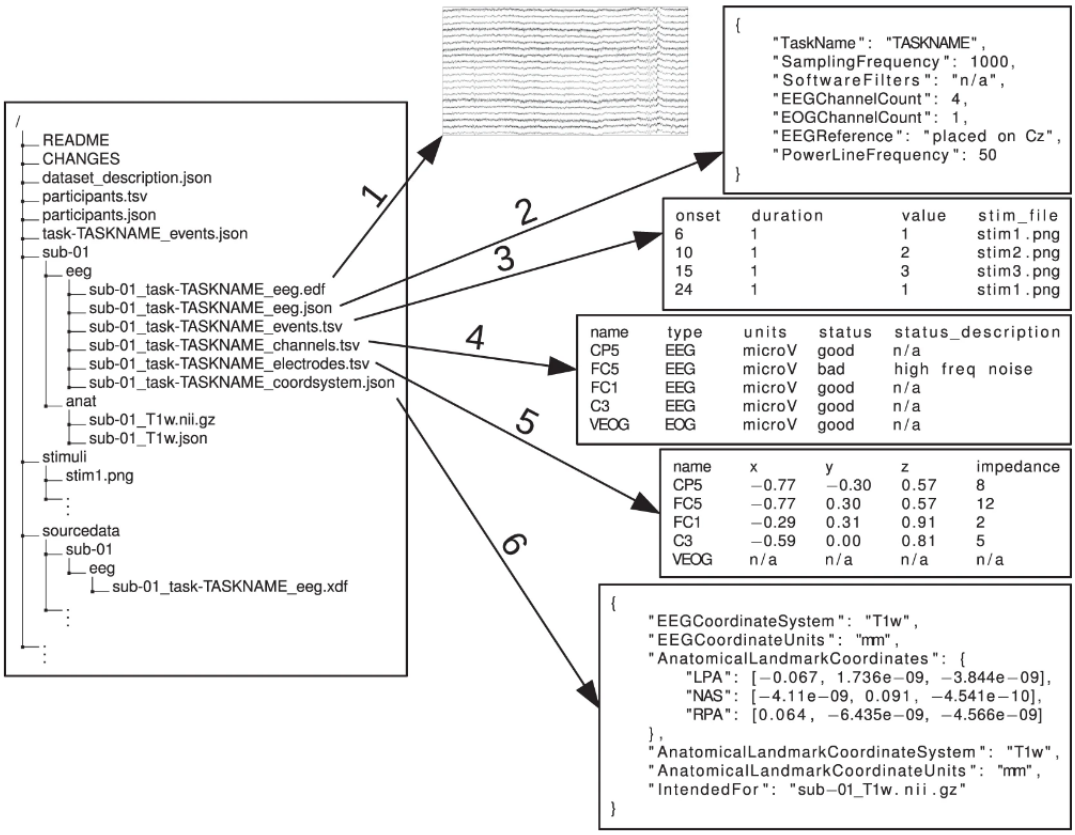

Figure 1: A file structure of the BIDS standard [1]

In the image above, a file structure of the BIDS standard is listed. The “README” and “dataset_description” files indicate general information about the dataset. In the " participants.tsv " file, the information of all patients or subjects is kept. In addition, there is also a "participants.json" file about the subjects . EEG records of each patient are kept in sub-xx files. The file extension of the EEG data could be bdf or edf. channels.tsv and electrots.tsv to specify which channels or electrodes are used while recording EEG signals. Thanks to BIDS, sharing and examining the data set has become very easy. Researchers who have a data set created with the BIDS standard can easily understand the information about the data set.

Hagiwara et al proposed an approach for the diagnosis of Parkinson's disease. This article proposes a system to automatically detect Parkinson's disease using a convolutional neural network (CNN) [2].

In this study, EEG data obtained from a total of 40 people, including 20 patients with Parkinson's disease and 20 healthy people, were used.

Records of Parkinson's patients were obtained from 10 male and 10 female subjects aged 45 to 65 years. In addition, the disease durations of these patients range from 1 to 12 years. Data from healthy people were obtained from 11 female and 9 male subjects who had no previous mental illness. Both healthy subjects and subjects with PD were right-handed. EEG recordings were taken at a sampling rate of 128GHz using the EPOC neuroheadset. While recording, the subjects were asked to sit down and avoid eye blinking or similar movements.

Each recordings took 5 minutes and the resulting recordings were divided into 2-second segments. The authors used at threshold technique to filter out the blinking artifacts. In addition, a Butterworth filter was used to filter the frequency range from 1 to 49 GHz. In this study, a thirteen-layer CNN structure was applied. As a result, the generated CNN model yielded 84.71% sensitivity, 88.25% accuracy and 91.77% specificity.

By Mohamed Shaban proposed an approach that performs Deep Learning-Based Automatic Screening of Parkinson's Disease [3].

In this article, a deep learning model using ANN applied only to Oz, FC2, P8 channels of EEG dataset is proposed. The data set was taken from 31 subjects. Sixteen of these subjects had Parkinson's disease and fifteen were healthy people. Eight female and eight male subjects of 16 patients had Parkinson's disease and they were right-handed. Nine of the data from healthy people were from women and six from men. All Parkinson's patients had mild or moderate disease phases. The data set was obtained using a total of fourty electrodes. The resulting data set was divided into 2-second segments consisting of 512 samples. The obtained EEG data was run using the ANN model consisting of 13 layers. ROC was used to evaluate the results obtained from the ANN model. As a result, 98% accuracy, 100% specificity and 97% sensitivity were obtained. It is envisaged to use CNN models to identify potential features in the future.

Vanegas et al. proposed an approach that examines biomarkers of Parkinson's disease with machine learning [4].

In this article, two different models are proposed for diagnosing Parkinson's disease from EEG data using machine learning methods. EEG data of 59 people were used. 29 of these EEG data were from Parkinson's disease and 30 of them were healthy people. EEG recordings were taken at a sampling rate of 1000 Hz. The EEG cap used while recording is a comprehensive cap that covers the head, neck, face and cheeks of the person and records in 256 channels. For this experiment, the electrodes on the neck, face and cheeks were removed from 256 channels and only the data collected by 185 electrodes on the head was used. Then, the obtained records were separated into 2240 ms parts and the Fourier Transform (FFT) was calculated. EEGLAB and topographic mapping were used to analyze the EEG data. When preprocessing was desired with the data obtained, the first and last 160 ms parts were not taken into account, and the

remaining 2240 ms parts were used in the experiment. In this study, each electrode was evaluated separately by using the Python Scikit Learning Toolbox in machine learning. 70% of all preprocessed data was used for train and 30% for testing purposes. The first model designed reached a high result with a classification performance of 0,95. The second model used a decision tree. Likewise, in the second model, 70% is reserved for train and 30% for testing. The second model achieved a classification performance of 0.86. Finally, in order to have the best classification performance, one hundred trees with a maximum depth of 30 and an extra tree were used. After 1000 iterations, a closest-perfect classification result of 0.99 was obtained.

Cahoon et al. a wavelet-based convolutional neural network (CNN) model is proposed for the detection of Parkinson's disease [5].

It is stated in the article that EEG data is not widely used in the detection of Parkinson's disease, but it gives high results with the latest developments. The data set used consists of two parts. Parkinson's patients were named PD, and healthy control people HC. The data set consists of EEG data from 31 test subjects. EEG data was acquired with a 32-channel neuro-cap. 4 of 32 channels were chosen randomly. These channels are FP1 FC1, CP5 and FZ. EEG signals received from these channels were converted to 24200 images with 128x128x1 size. All obtained data was trained over 40 epochs using a 13-layer CNN model with 4-fold cross-validation and 10-fold cross-validation. The results of the 4 channels used are presented separately. It was observed that the FP1 channel reached the lowest result with 0,97 among the channels, and the CP5 channel reached the highest result with 0,99. Very high-efficiency results were obtained in this study. However, it was stated by the authors that it is not suitable to be used for diagnosis without medical supervision.

Bragin et al. proposed a method for classification EEG signals images [6].

While making this classification, some situations such as the human condition and measurement accuracy were taken into account. It was stated that ANN, namely artificial neural networks, is a good tool to solve such problems. EEG signals are time series signals. For this reason, it is stated that Gramian Angular Field transform is used when transforming Images. It has been stated that CNN (convolutional neural networks) are used to classify electroencephalogram signals. The trigonometric sum of the values of each element at different time intervals is specified as the GAF, that is, the Gramian matrix. Grayscale images are used instead of color images in this article. The reason for using grayscale images is stated to increase the computation speed and reduce the number of neural network parameters. In this study, an EEG dataset consisting of 64 channels was used. The data set was obtained using the BCI-2000 system. The EEG dataset was recorded using a sampling frequency of 512Hz. The patient was asked to remain stationary while the data set was being recorded. Then, the subject was asked to perform some mental activities. All obtained records were converted to Gramian Angular Field images. Images are created in 128x128 size. In this study, a CNN model consisting of 4 layers was used. All the images obtained were trained and tested in the CNN model. As a result, the possibility of classification of EEG signals using Gramian Angular Field is examined in the article. The classification accuracy is 97%. It has been stated that better results can be obtained by using additional filters. Looking at the overall results, it has been observed that this method gives much higher results than other methods. It is stated that the presented method for classification of EEG signals can be used in a brain-computer interface.

Chapter 2

ELECTROENCEPHALOGRAPHY

Humans have billions of nerve cells in their nervous system. Most of these nerve cells are located in the brain. Every cell in the brain is in constant communication with other cells. This communication between the nerves leads to an electrical activity in the brain. EEG test is a method that allows the electrical activities in the brain to be measured with the help of a recording device. Recordings obtained by electroencephalography are called electroencephalogram, or EEG. This technique, called EEG, was first developed in 1929 by the German physician Hans Berger.

Electroencephalography (EEG) is the name given to the method of recording the electrical activity in the brain of electrodes attached to the scalp with or without hair. By using these electrodes detecting low-voltage electrical signals, electrical activity in every part of the brain can be easily recorded. Electrodes are small flat pieces of metal. The electrodes are attached to the scalp by means of a conductive gel. EEG waves may have peaks or troughs and doctors examining these recordings can tell if there is an abnormal signal when they look at lines of recordings. Irregular fluctuations in the waves are interpreted as abnormal situations. EEG is most commonly used in the diagnosis of epilepsy disease. However, it is also used in other neurological disfunctions such as Parkinson 's and Alzheimer diseases. During the EEG procedure, no electrical current is given to the patient and the patient does not feel any pain during EEG recording.

There is no harm in using the EEG test in pregnant women or young children. Hence, EEG test can be applied to individuals of all age groups as there are no side effects. Also, There is no harm in performing the EEG test frequently or for a long time. During the recording procedure, the patient may be asked to blink eyes, look at a fixed lamp, and breathe quickly for 3 minutes. An EEG test can be done while awake for a short time and the EEG test performed while awake is called routine EEG. Abnormal electrical activities that do not show up in a routine EEG test may occur during sleep. In order to detect these abnormalities.

EEG recordings can also be taken during sleep. It is known that some epileptic seizures occur only during sleep. For this reason, the EEG recording taken both while awake and while sleeping is considered the most accurate examination. This EEG recording is called "sleep-wake EEG". Some external factors affect the quality of the EEG recording. For example, while recording the EEG, the patient's hair should be clean and the patient's position should be comfortable and horizontal. Such factors affect the quality of the eeg recording positively or negatively.

Before the EEG recording, the head is measured by the technician. Next, the places where the electrodes should be attached are determined. All electrodes are adhered to the scalp using a conductive gel. In some cases, a cap to which the electrodes are attached may also be used. The amount of electrodes varies according to the cap used. The test can be performed using 12 to 64 electrodes. Below is an EEG- Cap image. It is possible to make more precise measurements by using EEG - Cap.

Figure 2: EEG – Cap [7]

Each electrode is called a channel, and each channel has a name. The most commonly used of these channels are FP1, FP2, F7, F3, Fz , F4, F8, T3, C3, Cz , C4, T4, T5, P3, Pz , P4, T6, O1 and O2. The anterior and posterior parts of the skull are defined as Nasion and Inion . Nasion represents the front of the skull. Inion refers to the back of the skull. When sticking the electrodes, it is ensured that they are always glued to the same place. Below are the images of two different electrode layouts, simple and detailed.

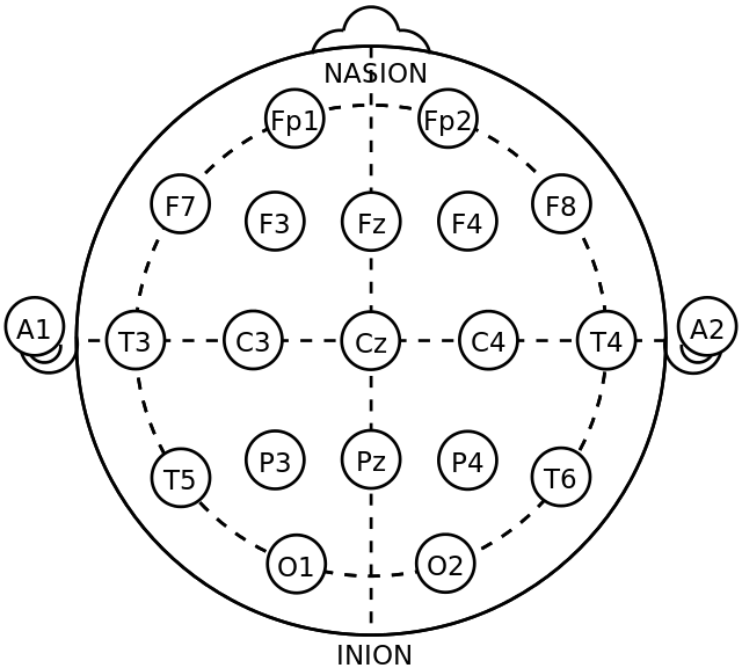

Figure 3: EEG simple electrode layouts[8]

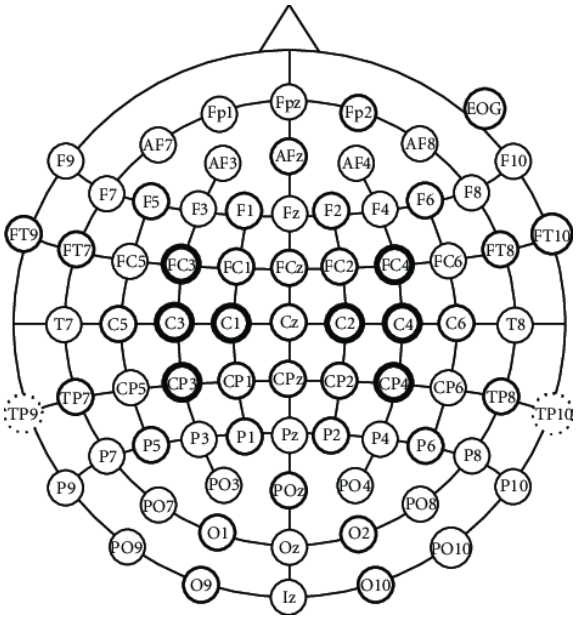

Figure 4: EEG Detailed electrode layouts[9]

After all the electrodes are connected to the computer. When the recording starts, the electrical activity in the brain starts to be registered recorded into a storage device.

It is ensured that the patient is in a comfortable position while recording. In order to increase the electrical activity in the brain while these recordings are being taken, the patient may be asked to do simple mathematical calculations or look at a picture.

During the EEG test, recordings can be taken at different frequencies. There are many different types of frequencies from 0 to 100 Hz. These frequency types and Hz ranges are listed in the table below.

Table 1: EEG test different frequency ranges

Type	**Frequency** (Hz)	Operation
Delta	0,5-3.5 Hz	In adults; Occurs in sleep mode.
Teta	4-7 Hz	In adults; arousal, laziness
Alfa	8-12 Hz	comfortable reflection close eyes
SMR	12-15 Hz	SMR
Beta	12-38 Hz	in alert work, busy, active or anxious thinking, effective concentration
Beta (Middle)	15-21 Hz	in alert work, busy, active or anxious thinking, effective concentration, normal concentration
Beta (High)	21-38 Hz	Stress, anxiety
Gamma	34-100+ Hz	certain motor brain functions

When the results of the EEG test completed, evaluations are made taking into account the drugs used and the age of the patient. Only a neurologist can make these evaluations. If the patient has a previous EEG test, the old and new test results are compared. If it is observed that the electrical activity in the brain is not in harmony, it is concluded that there may be a health problem related to the brain. Then, the disease caused by this incompatible electrical activity is determined by applying different test by associated experts.

Chapter 3

CONVOLUTIONAL NEURAL NETWORKS

With the latest developments in artificial intelligence, deep learning models that can perceive and classify like humans continue to develop day by day. Convolutional Neural Networks (CNN) is one of the most widely used deep learning-based algorithms for image classification and detection. Convolutional Neural Networks is a deep learning algorithm consisting of layers, Convolutional Layer (Relu), Pooling and Fully Connected layers.

ALexNet is a CNN architecture developed in 2012 by Alex Krizhevsky, Ilya Sutskever and Geoffrey Hinton. The 8-layer AlexNet architecture has proven itself by getting high results in the ImageNet Large-Scale Image Recognition Competition [10]. AlexNet was successful in the competition with an error rate of 15.3%. Of the 8 layers, 5 are "convolutional layers" and 3 are "fully connected" layers. The following image shows the AlexNet architecture.

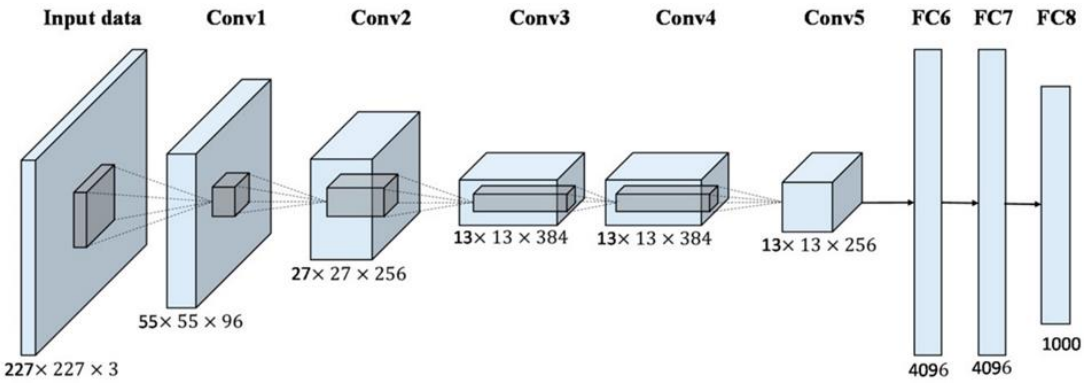

Figure 5: AlexNet Architecture [11]

AlexNet has a very similar structure to the LeNet architecture. [12] However, there are important differences. AlexNet architecture is much deeper than LeNet, while AlexNet consists of 8 layers, LeNet consists of 5 layers. AlexNet can show different actions in non-linear situations. Most standard neural networks used tanh or sigmoid. AlexNet uses ReLU as activation function instead of tanh or sigmoid. ReLU is more advantageous than sigmoid. It is advantageous because the model is faster when being trained.

As indicated in the image below, as the values of the sigmoid function get larger or smaller, its derivative approaches zero. This situation is called vanishing gradient. In this case, it becomes very difficult to update the weights. In deep models, this makes learning difficult.

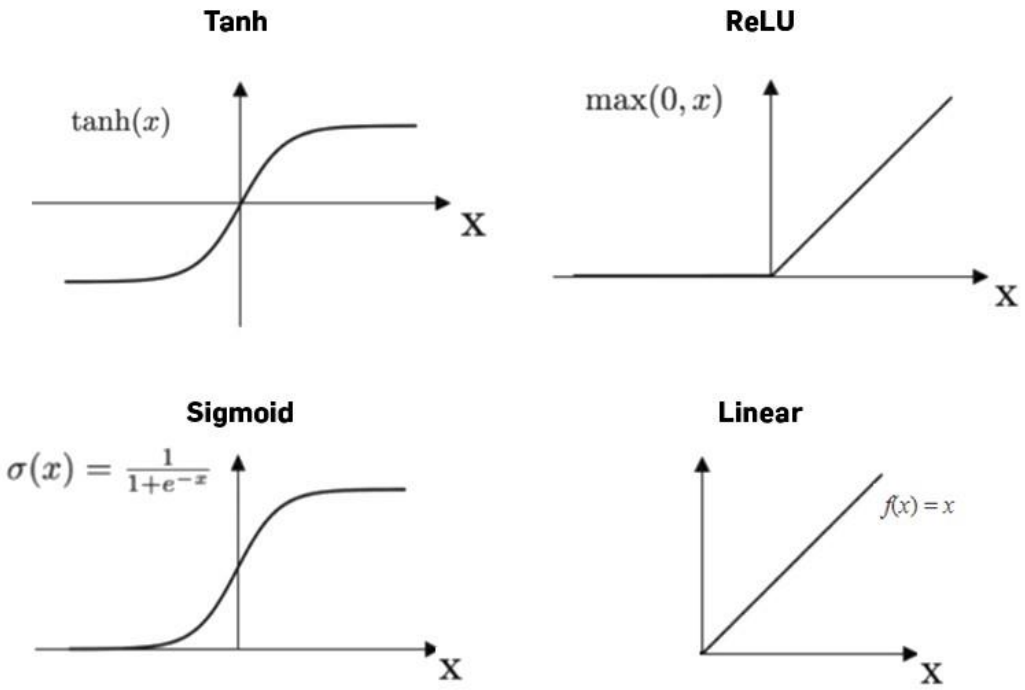

Figure 6: Tanh, ReLU, Sigmoid, Linear coordinate plane [13]

Another advantage of the AlexNet architecture is to avoid overfitting by using dropout. Overfitting is the memorization of the data given to the model for the train by the model. This problem can be summarized as training accurucy giving 99.5% and test accuracy 75.0%. In this case, it means that the model has not learned the data given for the train and has memorized it. AlexNet has prevented this by using dropout.

AlexNet consists of many parameters in total. Images can be given to the input layer of the network, such as 128x128x3 for example. The 3 here means RGB. The table below presents a table with AlexNet's layers and number of parameters.

AlexNet Network - Structural Details													
Input			Output			Layer	Stride	Pad	Kernel size		in	out	# of Param
227	227	3	55	55	96	conv1	4	0	11	11	3	96	34944
55	55	96	27	27	96	maxpool1	2	0	3	3	96	96	0
27	27	96	27	27	256	conv2	1	2	5	5	96	256	614656
27	27	256	13	13	256	maxpool2	2	0	3	3	256	256	0
13	13	256	13	13	384	conv3	1	1	3	3	256	384	885120
13	13	384	13	13	384	conv4	1	1	3	3	384	384	1327488
13	13	384	13	13	256	conv5	1	1	3	3	384	256	884992
13	13	256	6	6	256	maxpool5	2	0	3	3	256	256	0
						fc6			1	1	9216	4096	37752832
						fc7			1	1	4096	4096	16781312
						fc8			1	1	4096	1000	4097000
Total													**62,378,344**

Figure 7: AlexNet's layers and number of parameters

Chapter 4

GRAMIAN ANGULAR FIELD IMAGES

Gramian Angular Field is a time series encoding method. It was proposed by Zhiguang Wang and Tim Oates. GAF uses various operations to convert the time series data in the polar coordinate plane to the angular symmetry matrix. GASF or Gramian Angular Summation Field is a type of GAF.

Oates et al. proposed a framework for encoding time series as images, inspired by the recent achievements of deep learning in artificial intelligence [14].

In this study, three different methods are suggested. These methods are Gramian Angular Summation Field (GASF), Gramian Angular Difference Field (GADF), and Markov Transition Fields (MTF). These methods can be used in time series classifications and computer vision. Twenty standard datasets were used to test the three proposed methods. All data were tested on a CNN model. In order to determine the success rate of the proposed methods, they are compared with most of the best available time series classification methods. The results obtained are very promising. It is stated that it gives very good results compared to most existing methods.

Imaging Time Series

First, 2 separate frames are proposed to encode the time series as images. The first is a Gramian-Angular-Field (GASF) where time series are represented in a polar

coordinate system instead of Cartesian coordinates. In the Gramian matrix, each element corresponds to the cosine of the sum of the angles. In the second, Markov-Transition-Field (MTF) is proposed. The purpose of MTF is to construct the markov matrix after decomposition and encode the dynamic transition probability in the Gramian matrix.

Gramian Angular Field

First, all values of the time series are rescaled from 0 to 1 or from -1 to 1. The following formula was used for this process. Both formulas are used for scaling.

$$\tilde{x}^i_{-1} = \frac{(x_i - max(X) + (x_i - min(X))}{max(X) - min(X)}$$
$$\tilde{x}^i_0 = \frac{x_i - min(X)}{max(X) - min(X)}$$

Next, we can encode the 0 to 1 scale time series we get as the angular cosine and the timestamp as the radius. The following formula was used for this process.

$$\begin{cases} \phi = \arccos(\tilde{x_i}), -1 \leq \tilde{x_i} \leq 1, \tilde{x_i} \in \tilde{X} \\ r = \frac{t_i}{N}, t_i \in \mathbb{N} \end{cases}$$

The ti in this equation represents the timestamp. N is a constant value used for the polar coordinate system to improve the trajectory. This new polar-oriented system will be a new one for understanding time series. When the time value increasesi values are bent between different spaces in circles, like in a wave. There are two important features in this formula. cos(φ), φ ∈ [0, π]k is the monotonic bijective. Rescaled data has different angular boundaries. Gramian Angular Summation Field and Gramian Difference Field provide different levels of information granularity.The Gramian Angular Difference Field has the correct inverse map.

After converting the rescaled time series data to the polar coordinate system, we can easily take advantage of the angular perspective. Gramian-Angular-Summation-Field (GASF) and Gramian-Angular-Differential-Field (GADF) formulas are pictures.

$$\begin{aligned} GASF &= [\cos(\phi_i + \phi_j)] \\ &= \tilde{X}' \cdot \tilde{X} - \sqrt{I - \tilde{X}^2}' \cdot \sqrt{I - \tilde{X}^2} \end{aligned}$$

$$\begin{aligned} GADF &= [\sin(\phi_i - \phi_j)] \\ &= \sqrt{I - \tilde{X}^2}' \cdot \tilde{X} - \tilde{X}' \cdot \sqrt{I - \tilde{X}^2} \end{aligned}$$

GASF consists of 2 basic features. The first is to normalize the data in the range of 0 to 1. In other words, being able to transform GASF into normalized time series data using cross items. The second is to preserve absolute temporal relations with polar coordinates.

When converted to the polar coordinate system, the time series in each time step is taken as a one-dimensional metric space. GAFs have many advantages. As the position moves from top left to bottom right, they maintain temporal dependency. From the main diagonal, the time series can be reconstructed from high-level features learned by the deep neural network. GAFs are large relative to time series because they consist of nxn gramian matrices. It is possible to reduce this size.

The proposed method was compared with 9 different methods. For comparison, 20 different datasets were used. The results obtained are promising. It was stated that it gave very high results in 9 out of 20 datasets. Sufficiently high results were also obtained in the other 11 datasets.

Dataset	1NN-RAW	1NN-DTW-BWW	1NN-DTW-nWW	Fast-Shapelet	SAX-BoP	SAX-VSM	RPCD	SMTS	TSBF	GASF-GADF-MTF
50words •	0.369	0.242	0.31	N/A	0.466	N/A	0.2264	0.289	**0.209**	0.301 (16, 32)
Adiac ∗	0.389	0.391	0.396	0.514	0.432	0.381	0.3836	0.248	**0.245**	0.373 (32, 48)
Beef •	0.467	0.467	0.5	0.447	0.433	0.33	0.3667	0.26	0.287	**0.233 (64, 40)**
CBF †	0.148	0.004	0.003	0.053	0.013	0.02	N/A	0.02	**0.009**	**0.009 (32, 24)**
Coffee •	0.25	0.179	0.179	0.068	0.036	**0**	**0**	0.029	0.004	**0 (64, 48)**
ECG •	0.12	0.12	0.23	0.227	0.15	0.14	0.14	0.159	0.145	**0.09 (8, 32)**
FaceAll ∗	0.286	0.192	0.192	0.411	0.219	0.207	**0.1905**	0.191	0.234	0.237 (8, 48)
FaceFour ∗	0.216	0.114	0.17	0.090	0.023	**0**	0.0568	0.165	0.051	0.068 (8, 16)
fish ∗	0.217	0.16	0.167	0.197	0.074	**0.017**	0.1257	0.147	0.08	0.114 (8, 40)
Gun_Point ◁	0.087	0.087	0.093	0.061	0.027	0.007	**0**	0.011	0.011	0.08 (32, 32)
Lighting2 •	0.246	0.131	0.131	0.295	0.164	0.196	0.2459	0.269	0.257	**0.114 (16, 40)**
Lighting7 •	0.425	0.288	0.274	0.403	0.466	0.301	0.3562	**0.255**	0.262	0.260 (16, 48)
OliveOil •	0.133	0.167	0.133	0.213	0.133	0.1	0.1667	0.177	**0.09**	0.2 (8, 48)
OSULeaf ∗	0.483	0.384	0.409	0.359	0.256	**0.107**	0.3554	0.377	0.329	0.358 (16, 32)
SwedishLeaf ∗	0.213	0.157	0.21	0.269	0.198	0.01	0.0976	0.08	0.075	**0.065 (16, 48)**
synthetic control †	0.12	0.017	**0.007**	0.081	0.037	0.251	N/A	0.025	0.008	**0.007 (64, 48)**
Trace †	0.24	0.01	**0**	0.002	**0**	**0**	N/A	**0**	0.02	**0 (64, 48)**
Two Patterns †	0.09	0.0015	**0**	0.113	0.129	0.004	N/A	0.003	0.001	0.091 (64, 32)
wafer •	0.005	0.005	0.02	0.004	0.003	0.0006	0.0034	**0**	0.004	**0 (64, 16)**
yoga ∗	0.17	0.155	0.164	0.249	0.17	0.164	0.134	**0.094**	0.149	0.196 (8, 32)
#wins	0	0	3	0	1	5	3	4	4	**9**

Figure 8: GASF-GADF compared with 9 different methods

In conclusion, this article presents a set of formulas for converting to GASF, GADF and MTF images. A CNN model is used to test the performance of these methods. These methods, gave the most successful results in the application of many datasets compared to other methods. Using GASF, it has been shown to outperform raw data. It is foreseen that recurrent neural networks can be used in the future.

Chapter 5

K-FOLD CROSS VALIDATION

Cross-Validation is a statistical method that divides the data into many parts and enables train and test in different variations. [15] Each variation is compared and evaluated. In Cross-Validation, when creating train and test sets, each data segment is selected for training and testing in different variations. In this way, a crossover is made in successive rounds. The most basic of cross-validation is k-fold-cross-validation. In k-fold-cross-validation, the data is first segmented according to the given k value. For example, when k is selected as three, all data is split into three separate parts. Next, the first piece is reserved for testing and the other two pieces are used for the train. This is the first variation. In the second variation, the second piece is reserved for testing and the first and third pieces are used for training.

In the final variation, the third piece is reserved for testing and the first and second pieces are used for training. These 3 different variations are shown in the picture below. 3 separate boxes represent data. The light grey boxes represent the sections reserved for testing.

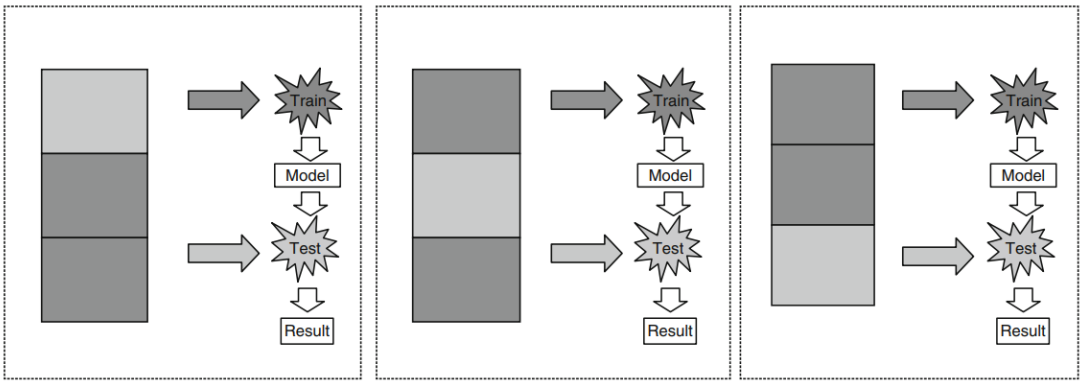

Figure 9: K-fold cross validation working logic [15]

In this way, not a single result, but a total of three results are obtained. Out of these three results using different variations, the one with the highest score is selected. In this way, it becomes possible to produce higher scores with different variations while training and testing, without relying on just one variation. The higher the K value is given, the higher the success rate will result. However, each time the value of k increases, the required processing load also increases. The main purpose of Cross-Validation is to evaluate and compare learning algorithms.

Chapter 6

METHODOLOGY

In this study, it is aimed for early diagnosis of Parkinson's disease by converting EEG data to GASF images, then train and test in a CNN architecture. In the literature, there are many studies that diagnosis Parkinson's disease using EEG data. However, no study was found using GASF. The main purpose of this study is to determine the success rate by comparing GASF with other studies. The reason for using GASF and CNN architecture in this study is that the success rate of CNN architecture in 2D images is quite high. In the studies, the success rate of CNN architecture in 2D images has been proven. For this reason, CNN is preferred as the neural network.

In this study, early diagnosis of Parkinson's disease was aimed using EEG data. EEG data collected by Alexander P. Rockhill, Nicko Jackson, Jobi George, Adam Aron, Nicole C. Swann UC San Diego Resting State EEG Data from Patients with Parkinson's Taken from the disease dataset. The data set consists of 6 versions in total. Versions have been updated over the years. The first version of the dataset was published on 05.05.2020. In this study, version v1.0.4 of the dataset published on 17.01.2021 is used. The data set consists of 328 files and has a total size of 545MB. The data set is shared so that it can be used free of charge. [16]. The dataset is organized in accordance with a previously proposed file structure.

A standard has been developed by researchers in the human brain imaging community to enable them to easily organize and share data. The name of this standard (BIDS) is The Brain Imaging Data Structure project. In this standard, unlike other standards, some general tools and references for EEG data are presented.

The BIDS EEG dataset extension closely follows the general BIDS specification. Each patient or subject's data is stored in subdirectories. At the top of the file structure there is a json file that gives general information about the dataset. This file is named dataset-description. The file, called eeg.json, provides comprehensive general information about the eeg registration system.

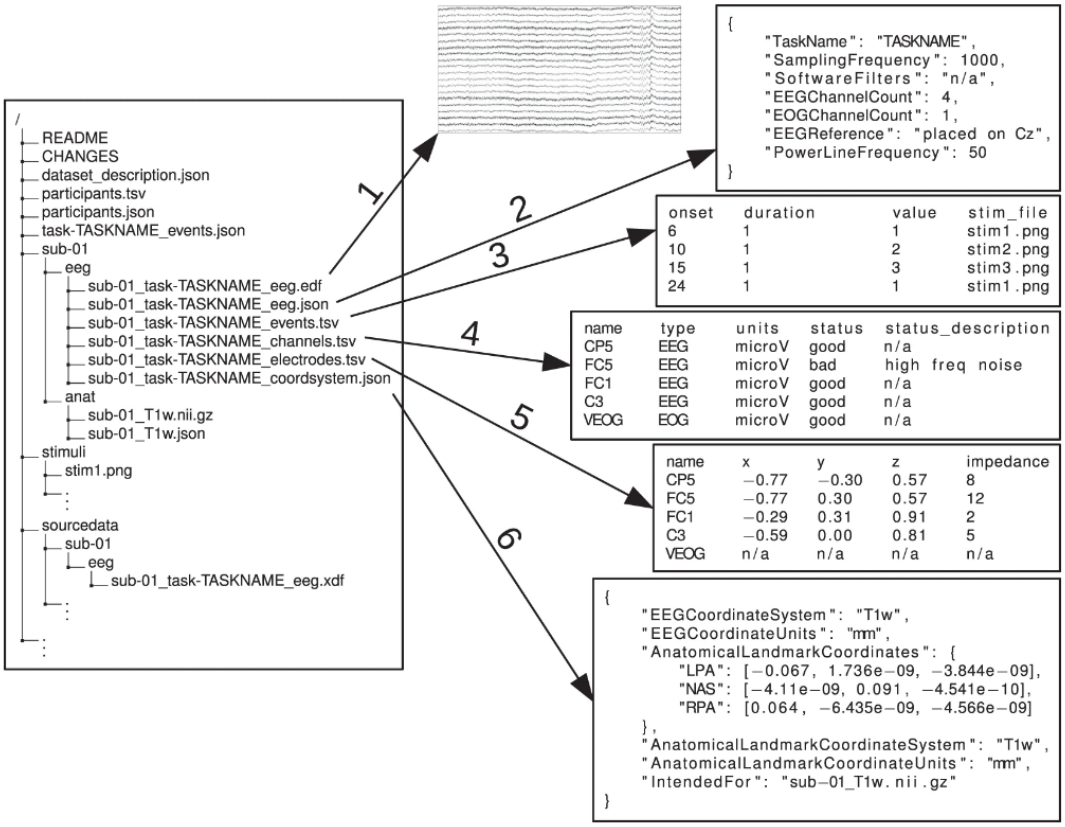

Figure 10: BIDS standard

In the image above, a file structure of the BIDS standard is listed. The “README” and “dataset_description” files indicate general information about the dataset. In the " participants.tsv " file, the information of all patients or subjects is kept. In addition, there is also a "participants.json" file about the subjects . The most important files are the subjects' files held as sub -xx. EEG records of each patient are kept in these files. The file extension of the EEG data is could be .bdf or .edf. channels.tsv and electrots.tsv to specify which channels or electrodes are used while recording EEG are kept in the files. Thanks to BIDS, sharing and examining the data set has become very easy. Researchers who have a data set created with the BIDS standard can easily understand the information about the data set [1].

6.1 Participants

The dataset was divided into two parts: have Parkinson's patients and healthy participants. Files of participants with Parkinson's disease were defined as PD. Data of healthy participants were defined as HC. The dataset was collected from 31 participants. Of these, 16 are healthy people and 15 are Parkinson 's patients. The data of 15 Parkinson's patients are kept in two files as PD-ON and PD-OFF. All participants are right-handed. Eight of the participants with Parkinson's disease were women and seven were men, and they were in the 55-71 age range. Nine of the healthy participants were women, seven were men and were between the ages of 54-73. Participants with Parkinson's were diagnosed by a movement disorder specialist at the Scripps clinic.

6.2 Data Collection

EEG data, BioSemi-ActiveTwo It was created non-invasively using the system. PD-ON and PD-OFF data were collected from subjects with Parkinson's disease at different times. PD-ON was collected from participants who had used a Parkinson's disease drug, namely dopaminergic medication, in the past 12 hours. PD-OFF, on the

other hand, keeps the EEG data of the same patients taken 12 hours before their medication was stopped. HC, that is, healthy participant data, was tested only once. While recording, the participants were asked to sit, stay still and look at an area on the screen. Extra electrodes were placed under and next to one eye to analyze movements such as blinking.

EEG data were collected from 32 channels and 512Hz samples. These channels are; FP1, AF3, F7, F3, FC1, FC5, T7, C3, CP1, CP5, P7, P3, PZ, PO3, O1, OZ, O2, PO4, P4, P8, CP6, CP2, C4, T8, FC6, FC2, F4, F8, AF4, FP2, FZ, CZ, EXG1, EXG2, EXG3, EXG4. These channels are marked in the image below.

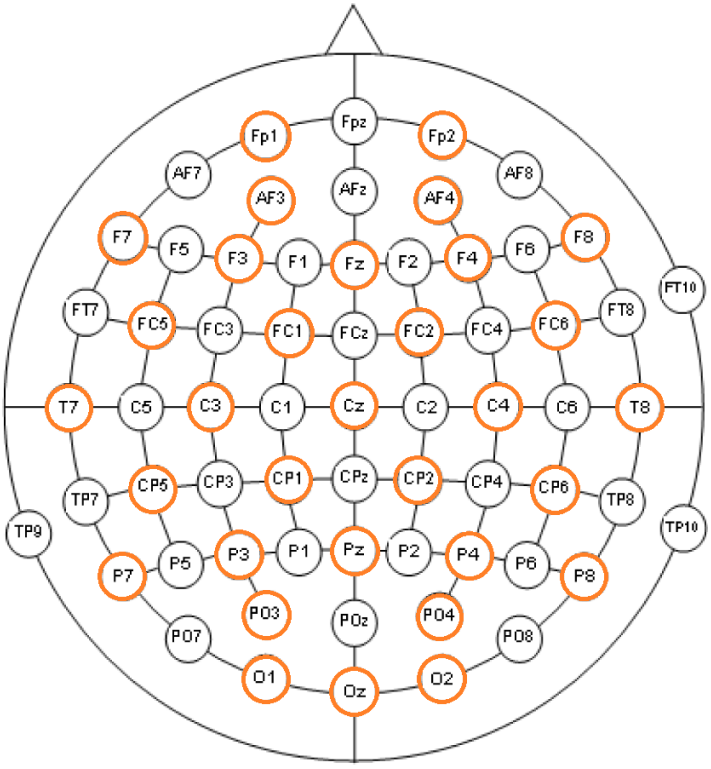

Figure 11: Channels available in the dataset used

6.3 Data Preprocessing

Data was processed in MATLAB using LetsWave6, LetsWave7 and EEGLAB functions. LetsWave custom scripts are used to monitor channels and signal lengths. Below are some of the images provided by the LetsWave7 plugin. In the images below, topograph and headplot images of HC, PD-ON and PD-OFF participants are given. In the pictures black dots represent channels and the colored parts represent the electrical activity in the brain. As seen in the bar graph next to the images, the blue colored areas represent areas in the brain where there is no electrical activity. The red areas are the areas where the electrical activity is most intense.

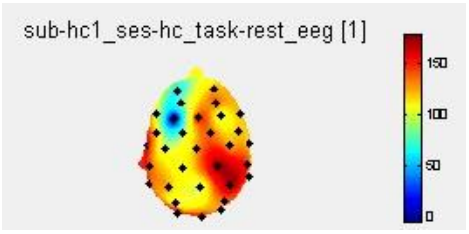

Figure 12: Headplot view with LetsWave7 HC

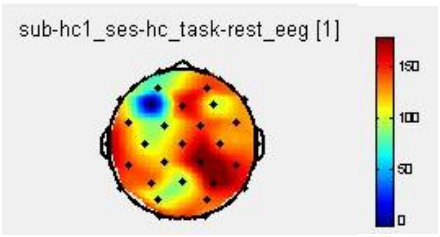

Figure 13: Topograph view with LetsWave7 HC

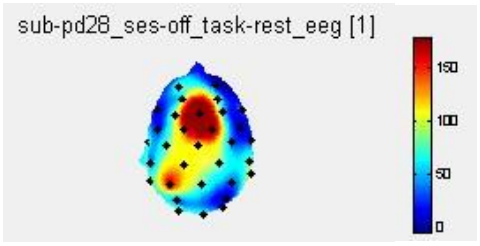

Figure 14: Headplot view with LetsWave7 PD-OFF

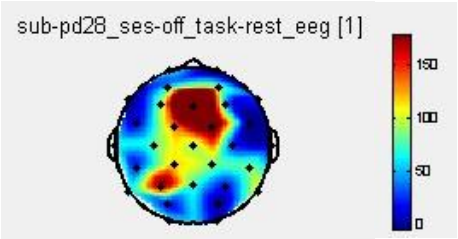

Figure 15: Topograph view with LetsWave7 PD-OFF

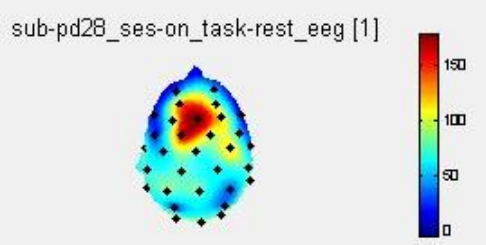

Figure 16: Headplot view with LetsWave7 PD-ON

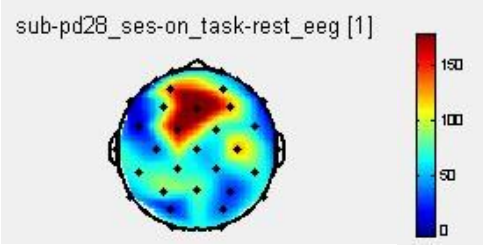

Figure 17: Topograph view with LetsWave7 PD-ON

Each of the eeg records in the dataset consists of records of at least 180 seconds (3 minutes). Records are not the same length. Some recordings are as long as 300 seconds. Below is the EEG recording of the HC-4 participant. In this image, all channels are listed under the channels title. As an example, the signal of the selected O1 channel is shown on the right side of the picture. Looking at the X-axis of the graph, it is observed that this record is collected in the range of approximately 0-181 seconds. Recordings were collected at 512Hz. That's why every second there are 512 samples. There are 92672 samples in total in this sample record. On the Y-axis of the graph, only the electrical activity of the O1 channel in the range of 0-170 is observed. The record in Image1 is filtered between 0 and 181. It started from 35 amplitude values

when recording started and reached 100 amplitude values at the tenth digit. It then decreased to 10 amplitude values at thirty-seventh seconds. As observed in the graph, the electrical activity reached its highest level between 94-96 seconds with an amplitude value of 170.

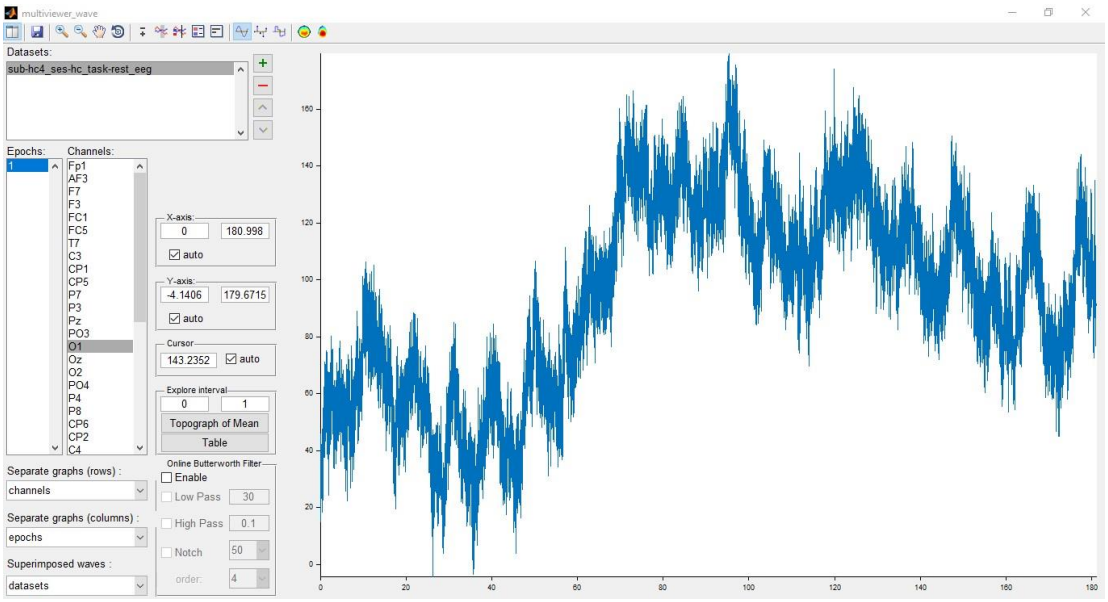

Figure 18: EEG recording of the HC-4 participant

0-1 range is examined by narrowing the filtering , it is observed that the amplitude value is approximately 35. In figure 19, there is a filtered version of the 0-1 range.

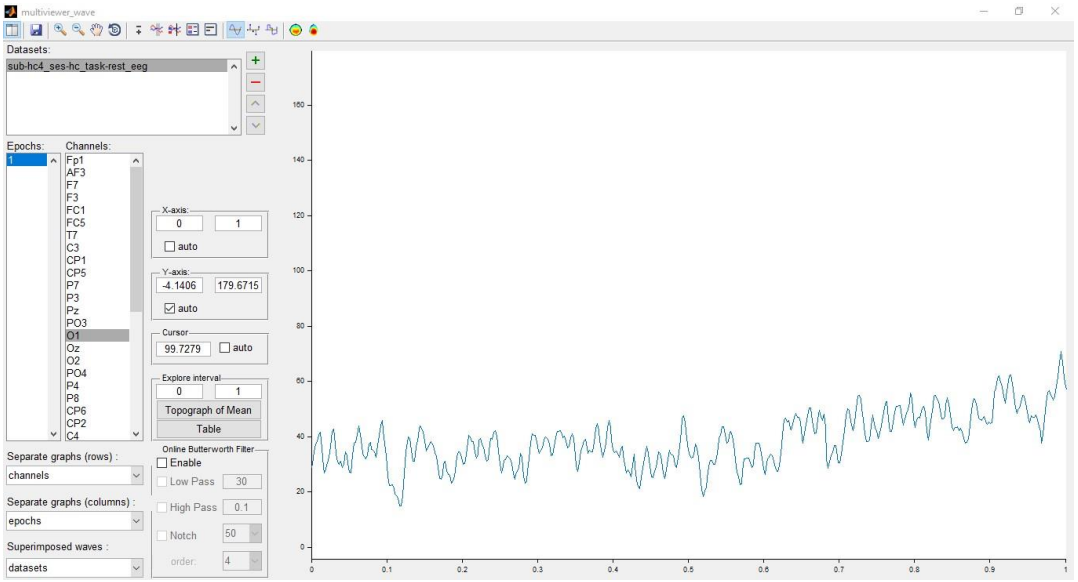

Figure 19: HC4 - filtered from 0-1 range of participant

When the filtering is narrowed and the range of 94-96 is examined, it is observed that the amplitude value is approximately 170. In figure 20, there is a filtered version of the range 94-96.

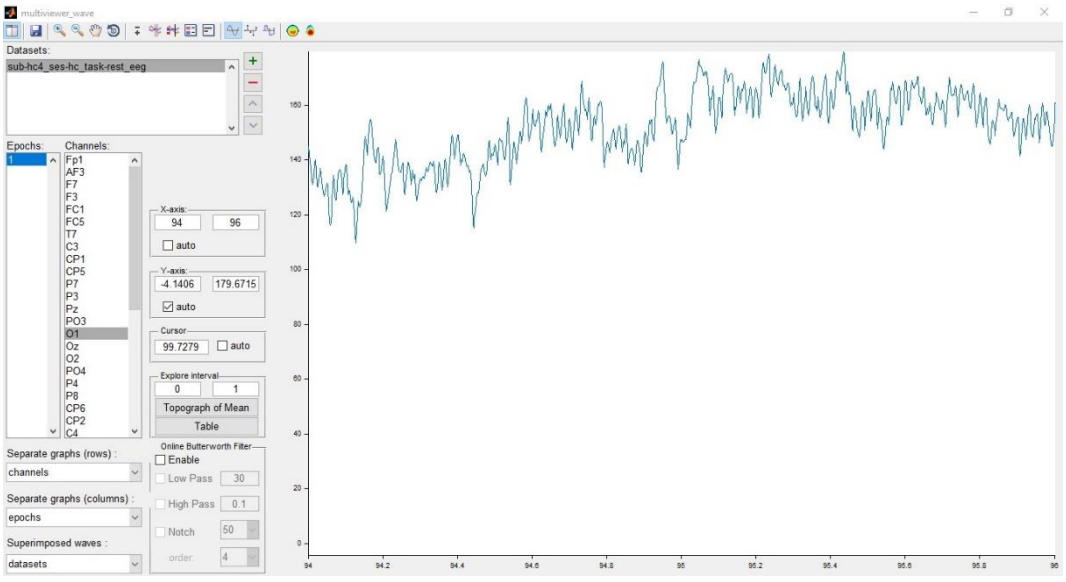

Figure 20: HC4 - filtered from 94-96 range of participant

LetsWave7 plugin does not allow us to export this data in csv format. Therefore, EEGLAB and MATLAB programs were used to export the data in csv format. The

reason for using both LetsWave7 and EEGLAB is to analyze whether the data has been corrupted during import. In order to analyze these differences that may occur in both programs, the O1 channel of the HC4 participant was selected and compared. As can be seen in the figüre 12 below, the O1 channel data of the HC4 participant consists of 180,998 seconds in total, approximately 3 minutes. As observed in Letswave7, it consists of 92672 samples in total with 512Hz.

Figure 21: The O1 channel data of the HC4 participant

When the O1 channel of the HC4 participant is analyzed graphically using EEGLAB, the same results are observed with LetsWave7. In the following figure 22, the filtered graph between 0-5 seconds is presented in the graph. It was observed that the

amplitude value was 34.5468 by 0.0041262. According to these results, both programs gave the same results. Analysis can be done from both programs.

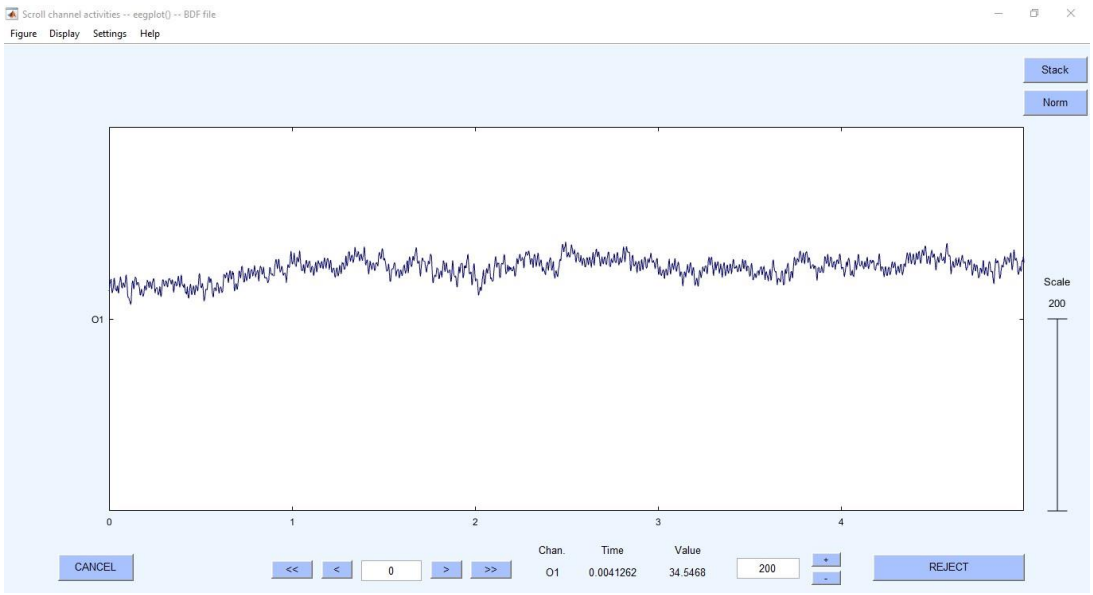

Figure 22: Figure 20: HC4 - filtered from 0-5 range of participant

After verifying the accuracy of the programs, the data of the O1 channel of the HC4 participant were exported via the EEGLAB program to be converted to csv format. Then it was converted to csv format with matlab. The data to be converted to csv format was transferred to the matlab program. O1 channel results of HC4 participant are presented in figure 23.

Time	O1
NUMBER	NUMBER
Time	O1
0.0000	28.7968
1.9531	30.4531
3.9063	34.5468
5.8594	37.4218
7.8125	38.3281
9.7656	40.8593
11.7188	41.7968
13.6719	35.9843
15.6250	28.9218
17.5781	27.0156
19.5313	28.4531
21.4844	30.5781
23.4375	32.5156
25.3906	36.7031
27.3438	42.0468
29.2969	42.8280
31.2500	37.5156
33.2031	33.7343
35.1563	30.7968
37.1094	30.0156
39.0625	31.0468
41.0156	28.8281
42.9688	30.3281

Figure 23: O1 channel results of HC4 participant

Amount of samples in each GASF image to be created to be 512, all data was read in the created matlab program and converted to csv file by the program created with 512 samples in each line. A csv file consisting of 92672 / 512 = 181 lines was created for the O1 channel of the HC4 participant.

All of the mentioned transactions were made separately for each channel belonging to all participants. Then, csv files were created by combining all the data on a channel basis, including HC, PD-ON and PD-OFF.

CSV files were read separately by creating a program in CSV python language. Since there are negative and positive values for some channels in the values in the csv file read, first of all, all values are placed in the 0-1 range. Then, the values in the 0-1 range created were converted to GASF images.

A GASF image was generated for each 512 consecutive samples. The images were adjusted to be 128x128, taking into account the image sizes in similar studies. [2][3][4][5][17].

Three separate folders were created for each channel: HC, PD-ON and PD-OFF. Since there are 36 channels in total to be used in the train and test of the model, 36 separate folders have been created. Channel names are given to these folders. Folders are made ready for training and testing.

All images that have been prepared are intended to be trained with a model. At this stage, it is desired to choose the most suitable neural network among many neural networks. Many articles have been reviewed on this subject.

Angelin Sarah et al. have presented a comprehensive article examining deep learning techniques related to EEG signal applications.[17] In this context, 156 articles on deep learning-based EEG applications between 2010 and 2018 were reviewed. This article provides an understanding of deep learning-based EEG applications and neural networks for various purposes. Many different network types and algorithms have been examined about deep learning. These; CNN, RNN, AE, RBM, MLPNN and DBN. In this article, It has been stated that Convolutional Neural Networks (CNN) are successful in processing nonlinear data. Also, It has been stated that convolutional

neural networks give better results than recurrent neural networks in classifying EEG data. In the researches on CNN, accuracy, sensitivity and specificity rates of 15 different methods are presented. In these studies, 5-13 layered architectures were used. In addition, studies on RNN, AE, RBM and DBN and the results of these studies are presented. As a result, it was stated that convolutional neural networks, recurrent neural networks and deep belief networks performed better in EEG data. In particular, it has been stated that CNN and RNN have the highest performance rate in image recognition and nonlinear signals.

As a result of the researches, it has been understood that Convolutional Neural Networks are more successful than other neural networks in processing nonlinear data and image recognition. For this reason, the Convolutional neural network model is used.

Chapter 7

RESULTS AND DISCUSSIONS

7.1 Preparation of the Working Environment

HC, PD-ON and PD-OFF folders were created by combining the data of all channels. AlexNet model was created to perform train and test operations. It is desired to perform train and test operations using AlexNet model with these images on various personal computers. These images were tried to be processed with the CPU on personal computers. However, it was not possible to train and test all the data due to the slow and insufficient processing power of the CPU in image processing. Later, in the researches, it was understood that the GPU is faster in image processing [18][19][20]. GPU-Tensorflow, GPU-Keras, CUDNN and CudaToolkit have been installed on personal computers so that these operations can be done over the GPU. However, due to insufficient memory capacity of GPUs in personal computers, it was not possible to operate with GPU. For this reason, the search for a virtual machine was started and the Google Colab pro version, which belongs to Google, was rented. Google Colap pro version provides GPU, TPU and high memory usage. All images are uploaded to Google Drive so they can be read through Google Colab pro. Two separate problems were encountered when trying to train and test using all images via Google Colab. First of all, because there are many images, the request to read the images times out. The other problem is that Google Cloab's GPU and memory capacity is insufficient for all images. There is only one possibility left. It is training and testing by selecting only some channels, not all channels. Some studies on this subject have been examined. In

these studies, it was understood that these processes were carried out by selecting 3 or 4 channels. Channel selection is randomly selected in some articles. However, in some studies, all channels were trained and tested one by one and the channels with the highest results were selected. At this stage, 16 of the 36 channels were randomly selected. After that, all channels were trained and tested one by one to observe the results of all selected channels. The list of these 16 channels selected are: Fp1, F7, F3, C3, P3, Pz, O1, Oz, O2, P4, C4, F4, F8, Fp2, Fz, Cz. Selected channels are shown in figüre 24.

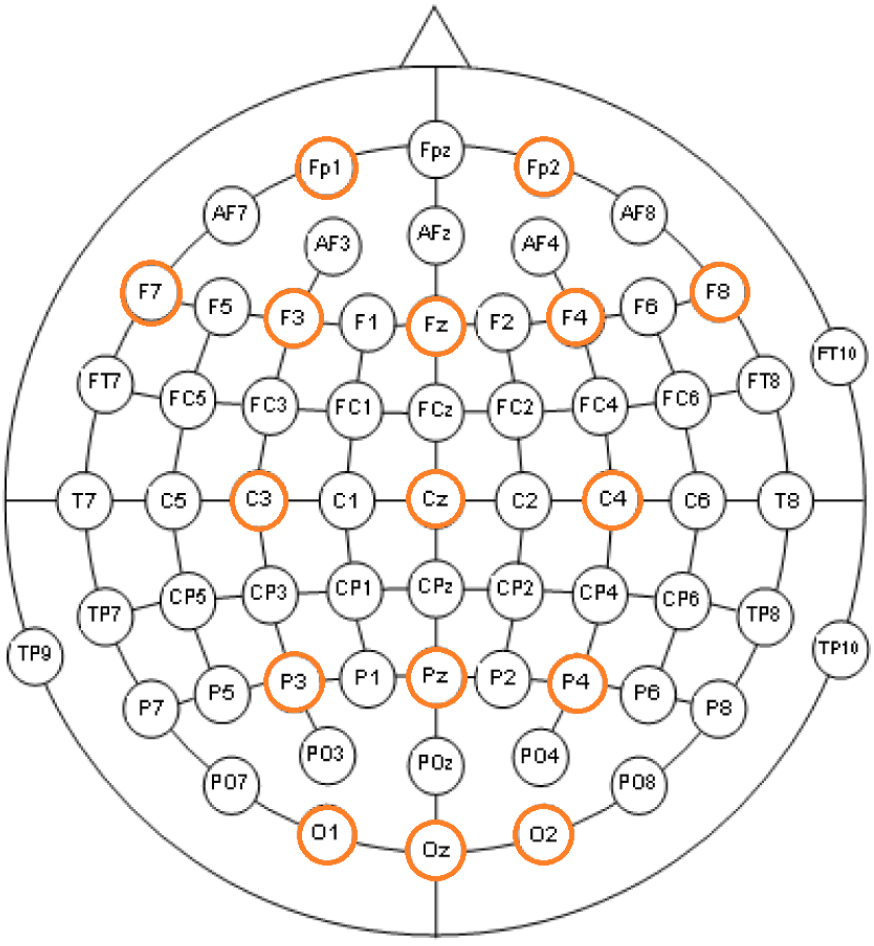

Figure 24: Selected channels for train and test

Below are the results obtained for all selected channels.

7.1.1 EEG Channel Fp1

The data of the Fp1 channel are divided into HC and PD-ON. Then, it was trained and tested using AlexNet deep learning model and Google Colab. Obtained results are presented below.

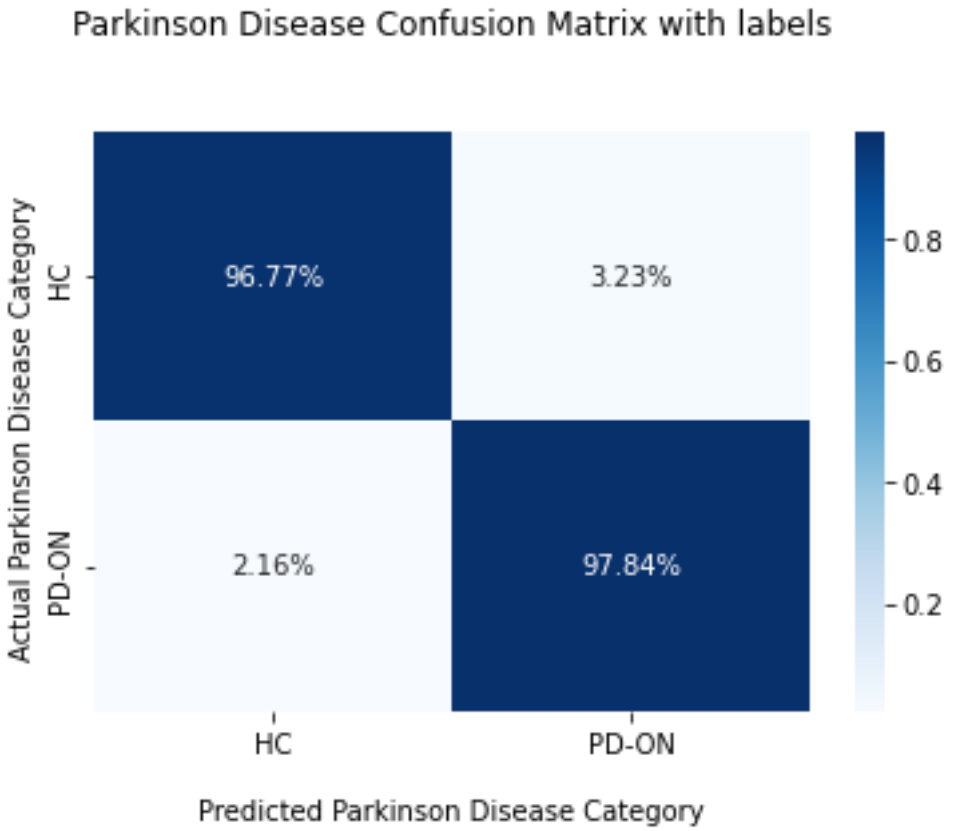

Figure 25: Fp1 channel HC and PD-ON Confusion Matrix

Accuracy = 0. 9729166666666667

Sensitivity = 0. 978448275862069

Specificity = 0. 967741935483871

The data of the Fp1 channel are divided into HC and PD-OFF. Then, it was trained and tested using AlexNet deep learning model and Google Colab. Obtained results are presented below.

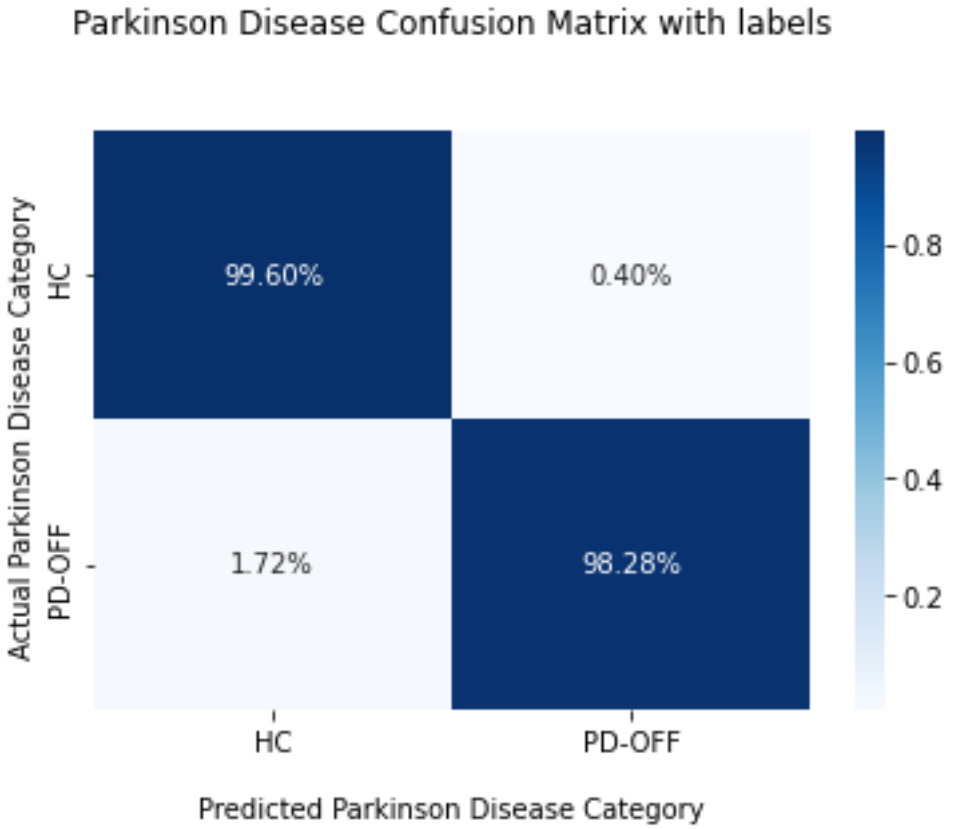

Figure 26: Fp1 channel HC and PD-OFF Confusion Matrix

Accuracy = 0.9895833333333334

Sensitivity = 0.9827586206896551

Specificity = 0.995967741935483

7.1.2 EEG Channel F7

The data of the F7 channel are divided into HC and PD-ON. Then, it was trained and tested using AlexNet deep learning model and Google Colab. Obtained results are presented below.

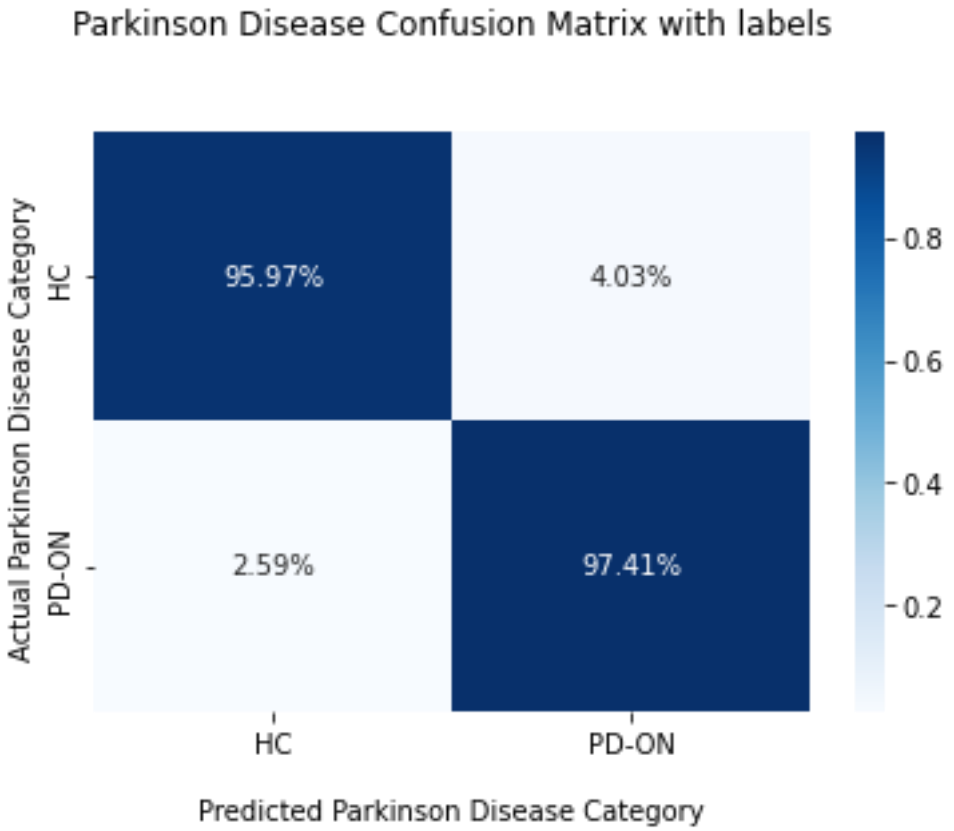

Figure 27: F7 channel HC and PD-ON Confusion Matrix

Accuracy = 0. 9666666666666667

Sensitivity = 0. 9741379310344828

Specificity = 0. 9596774193548387

The data of the F7 channel are divided into HC and PD-OFF. Then, it was trained and tested using AlexNet deep learning model and Google Colab. Obtained results are presented below.

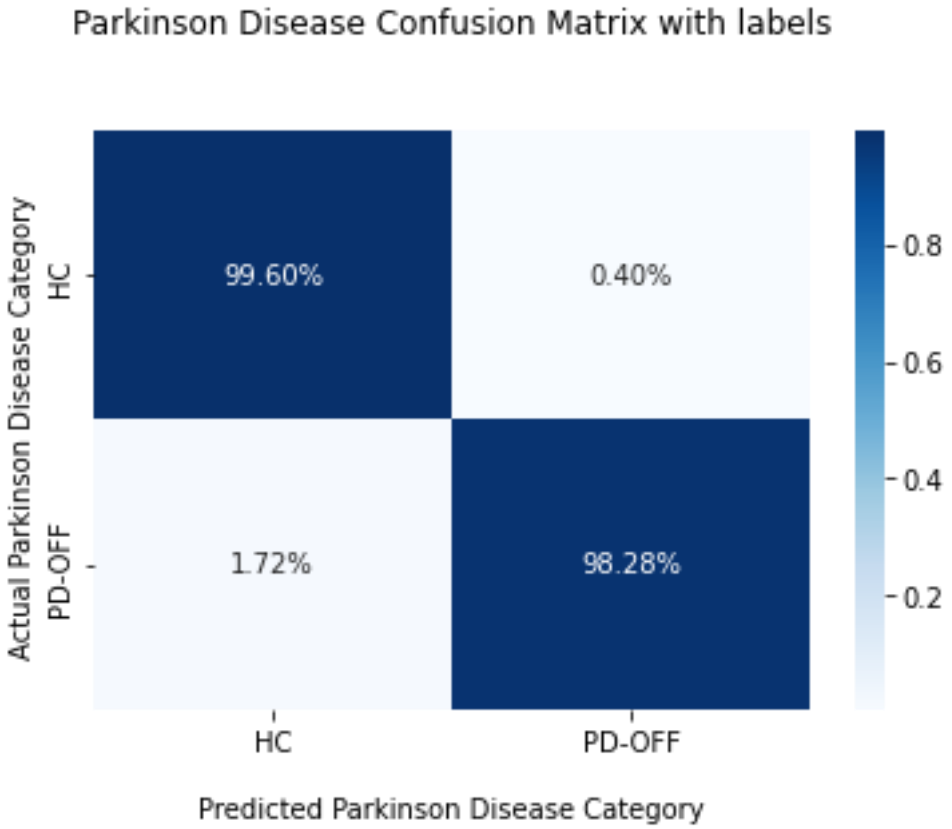

Figure 28: F7 channel HC and PD-OFF Confusion Matrix

Accuracy = 0.9895833333333334

Sensitivity = 0.9827586206896551

Specificity = 0.9959677419354839

7.1.3 EEG Channel F3

The data of the F3 channel are divided into HC and PD-ON. Then, it was trained and tested using AlexNet deep learning model and Google Colab. Obtained results are presented below.

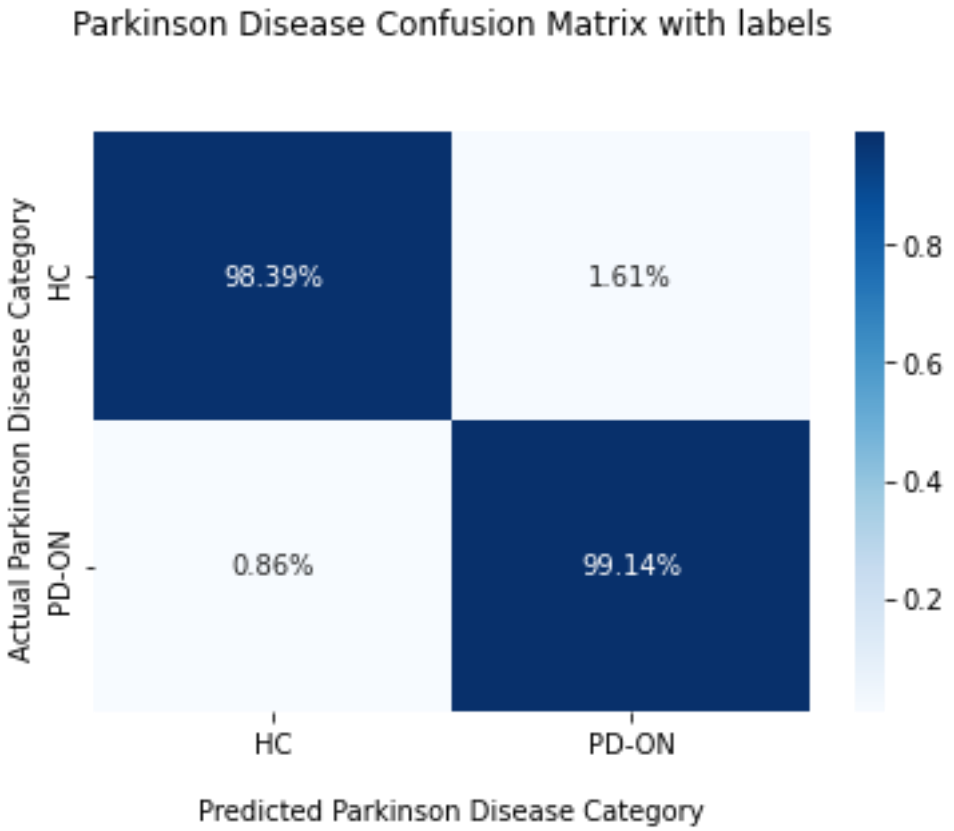

Figure 29: F3 channel HC and PD-ON Confusion Matrix

Accuracy = 0. 9875

Sensitivity = 0. 9913793103448276

Specificity = 0. 9838709677419355

The data of the F3 channel are divided into HC and PD-OFF. Then, it was trained and tested using AlexNet deep learning model and Google Colab. Obtained results are presented below.

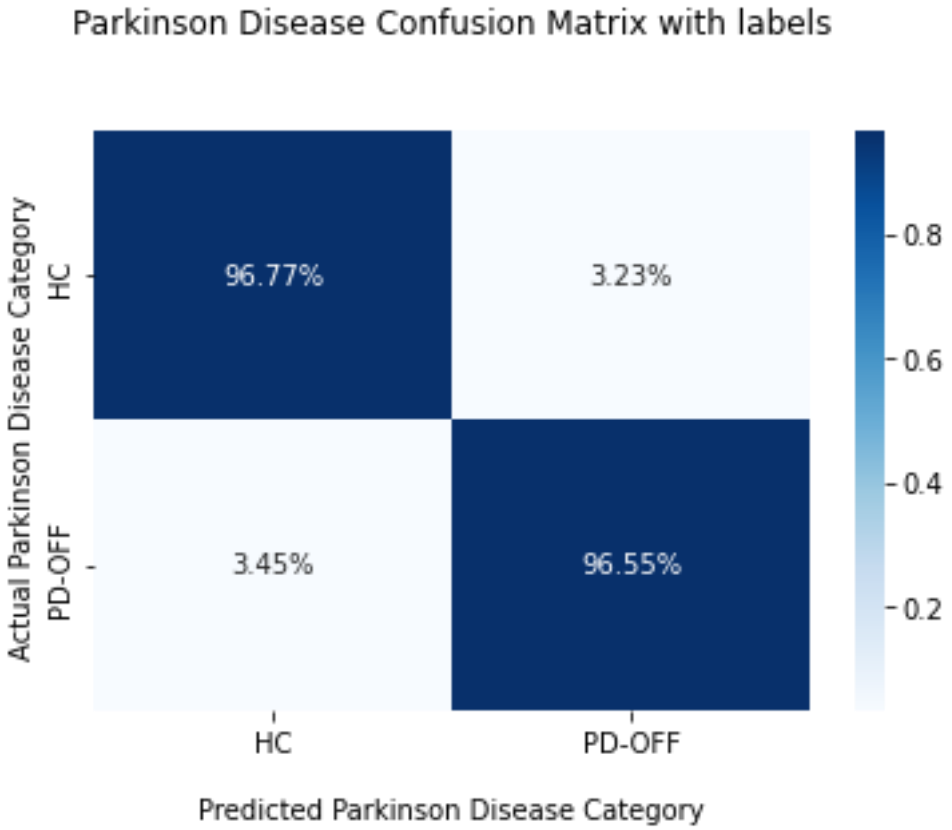

Figure 30: F3 channel HC and PD-OFF Confusion Matrix

Accuracy = 0. 9666666666666667

Sensitivity = 0. 9655172413793104

Specificity = 0. 967741935483871

7.1.4 EEG Channel C3

The data of the C3 channel are divided into HC and PD-ON. Then, it was trained and tested using AlexNet deep learning model and Google Colab. Obtained results are presented below.

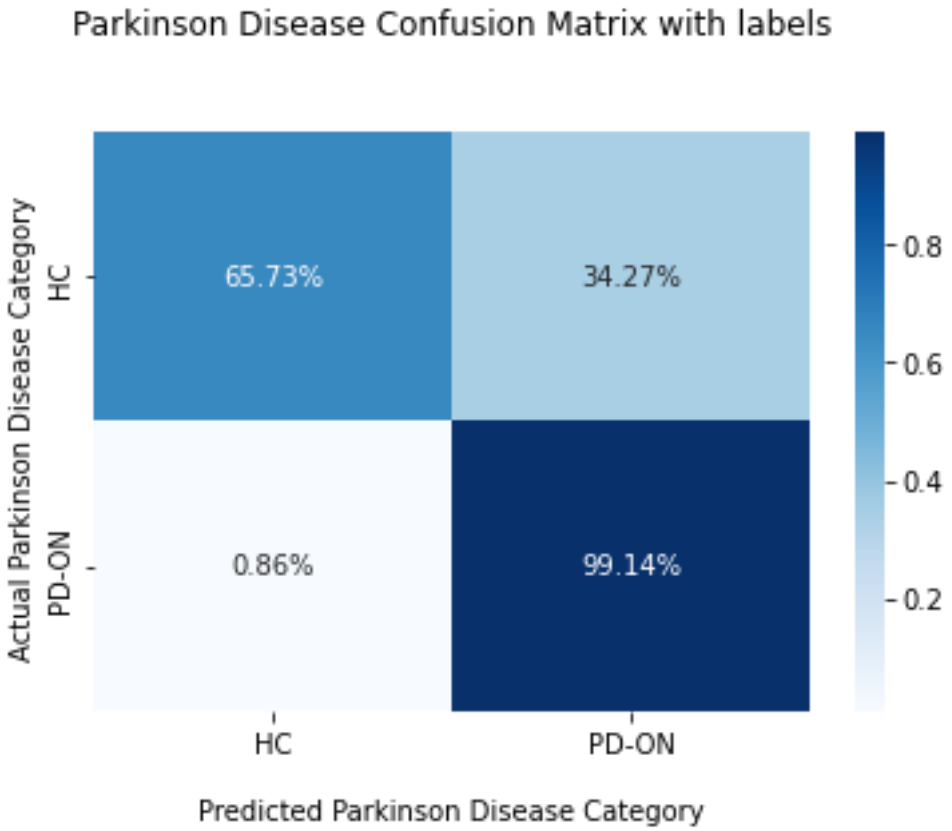

Figure 31: C3 channel HC and PD-ON Confusion Matrix

Accuracy = 0.81875

Sensitivity = 0.9913793103448276

Specificity = 0.657258064516129

The data of the C3 channel are divided into HC and PD-OFF. Then, it was trained and tested using AlexNet deep learning model and Google Colab. Obtained results are presented below.

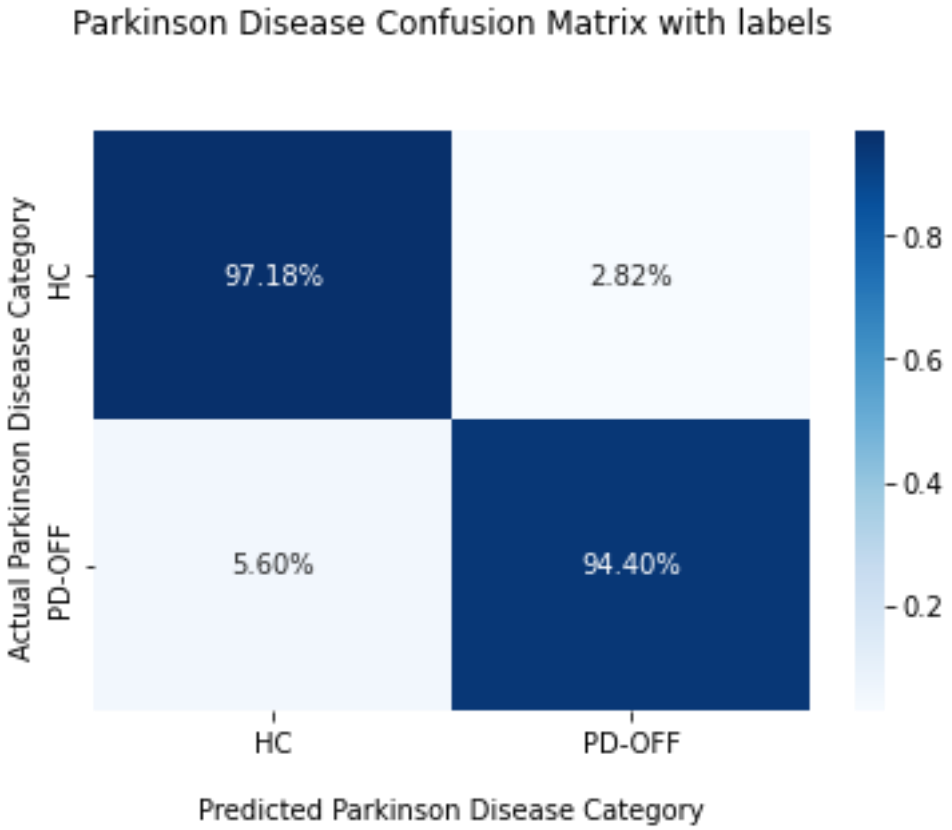

Figure 32: C3 channel HC and PD-OFF Confusion Matrix

Accuracy = 0. 9583333333333334

Sensitivity = 0. 9439655172413793

Specificity = 0. 9717741935483871

7.1.5 EEG Channel P3

The data of the P3 channel are divided into HC and PD-ON. Then, it was trained and tested using AlexNet deep learning model and Google Colab. Obtained results are presented below.

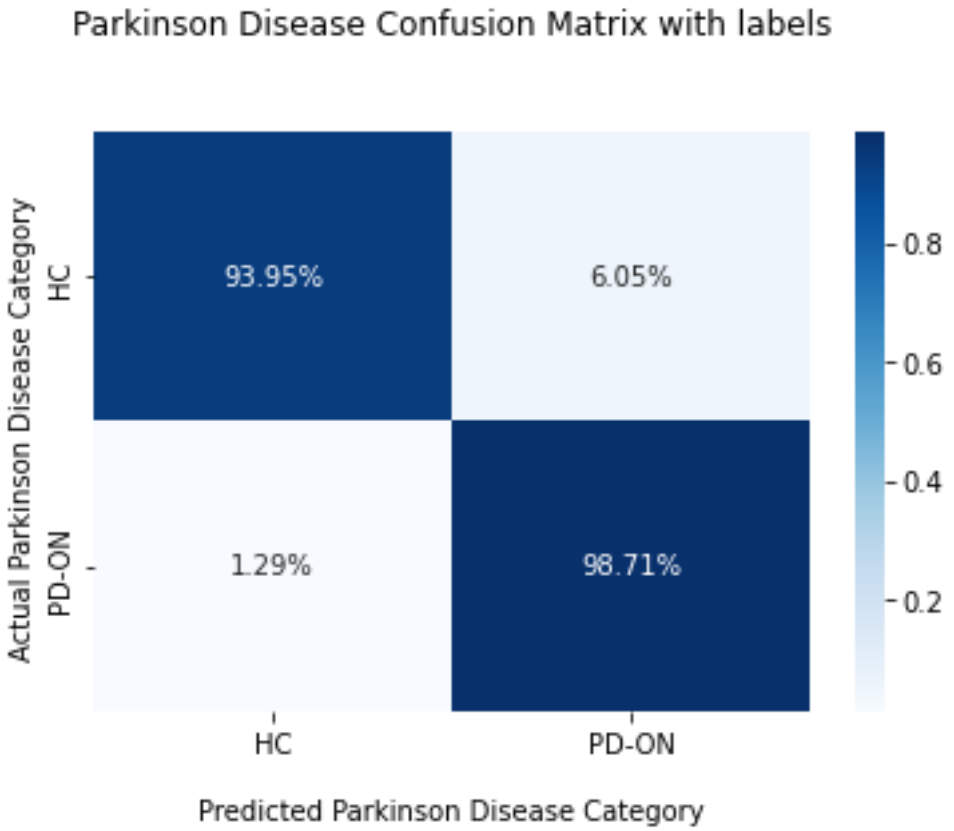

Figure 33: P3 channel HC and PD-ON Confusion Matrix

Accuracy = 0. 9083333333333333

Sensitivity = 0. 9913793103448276

Specificity = 0. 8306451612903226

The data of the P3 channel are divided into HC and PD-OFF. Then, it was trained and tested using AlexNet deep learning model and Google Colab. Obtained results are presented below.

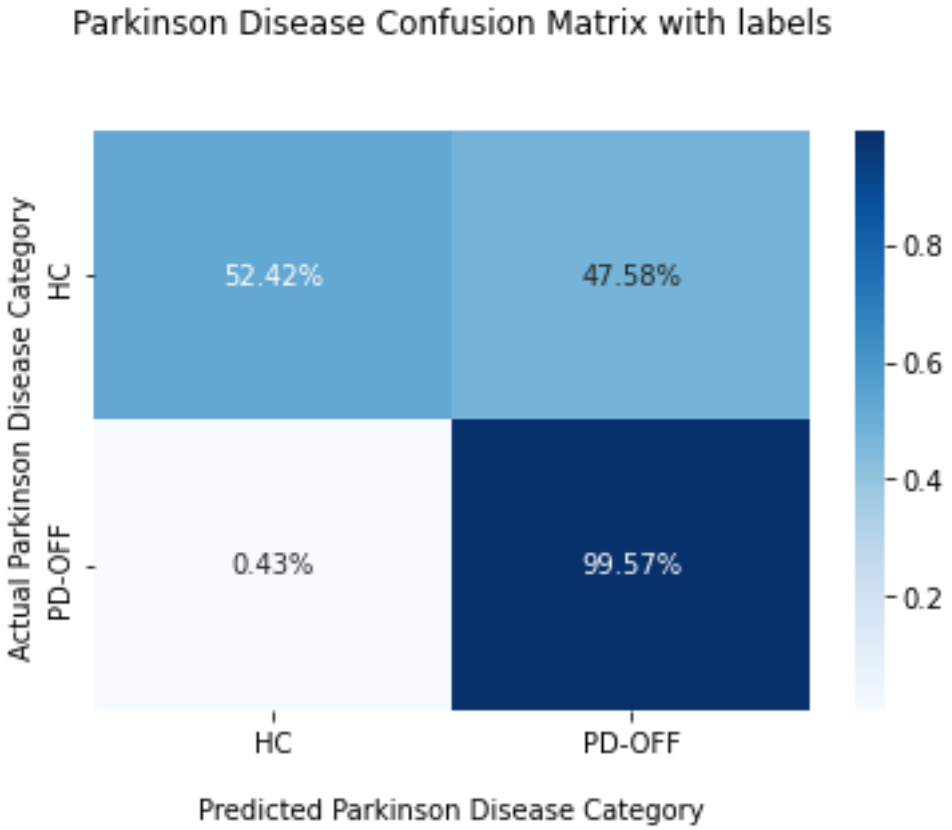

Figure 34: P3 channel HC and PD-OFF Confusion Matrix

Accuracy = 0. 7520833333333333

Sensitivity = 0. 9956896551724138

Specificity = 0. 5241935483870968

7.1.6 EEG Channel Pz

The data of the Pz channel are divided into HC and PD-ON. Then, it was trained and tested using AlexNet deep learning model and Google Colab. Obtained results are presented below.

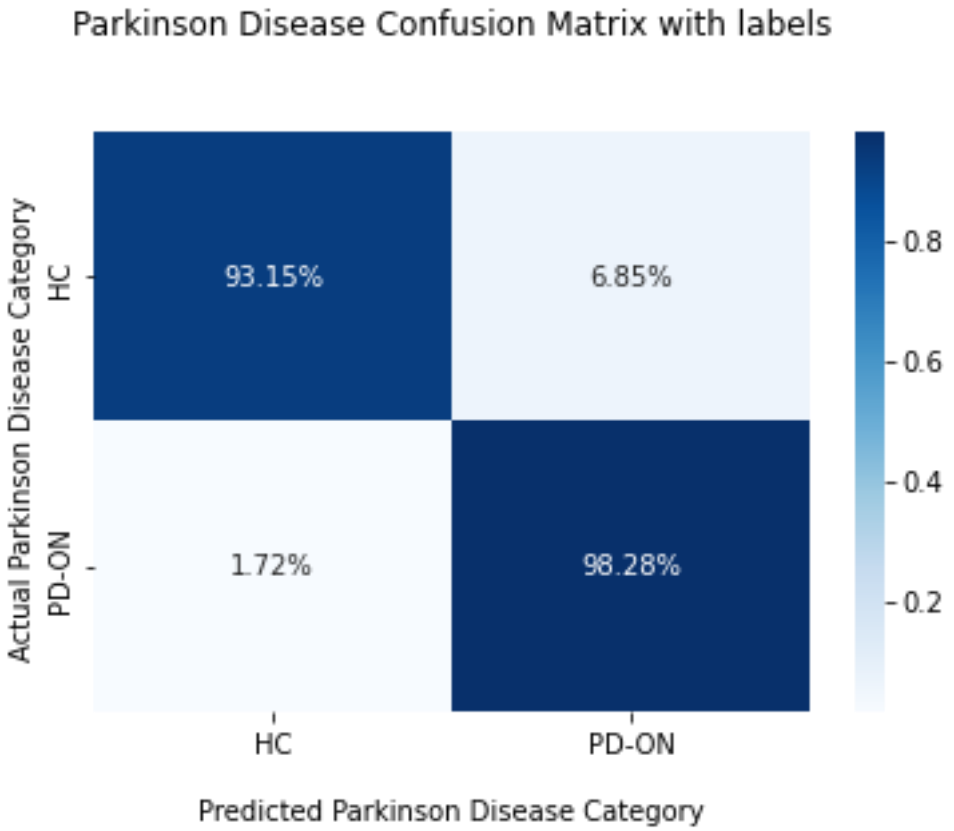

Figure 35: Pz channel HC and PD-ON Confusion Matrix

Accuracy = 0. 95625

Sensitivity = 0. 9827586206896551

Specificity = 0. 9314516129032258

The data of the Pz channel are divided into HC and PD-OFF. Then, it was trained and tested using AlexNet deep learning model and Google Colab. Obtained results are presented below.

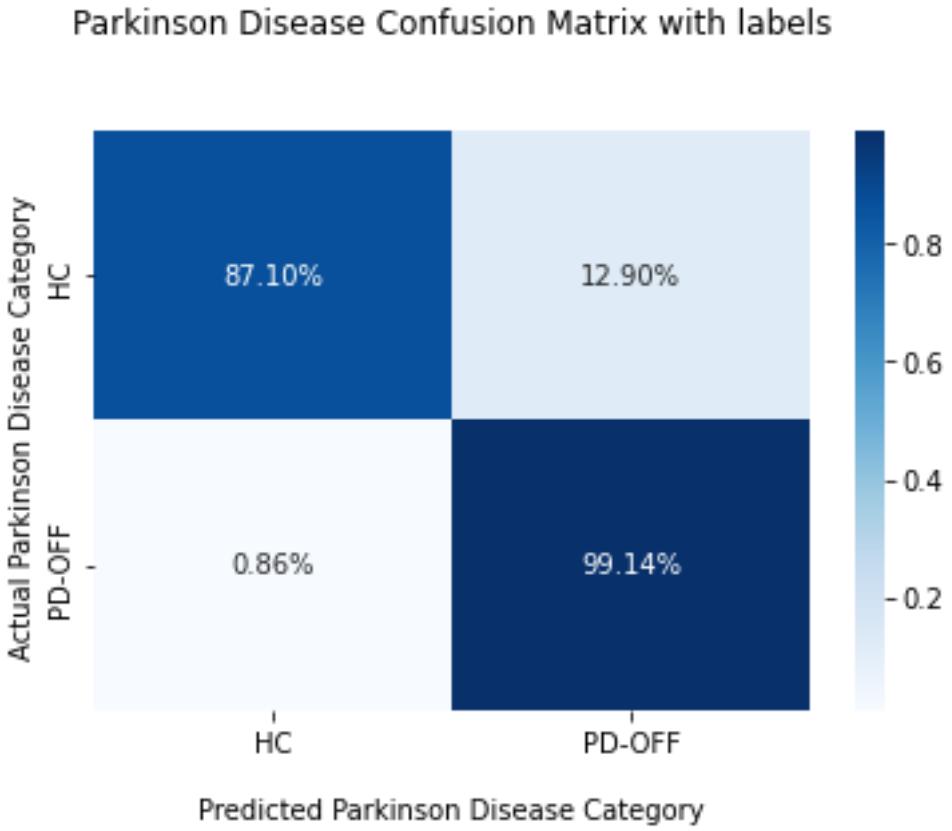

Figure 36: Pz channel HC and PD-OFF Confusion Matrix

Accuracy = 0. 9291666666666667

Sensitivity = 0. 9913793103448276

Specificity = 0. 8709677419354839

7.1.7 EEG Channel O1

The data of the O1 channel are divided into HC and PD-ON. Then, it was trained and tested using AlexNet deep learning model and Google Colab. Obtained results are presented below.

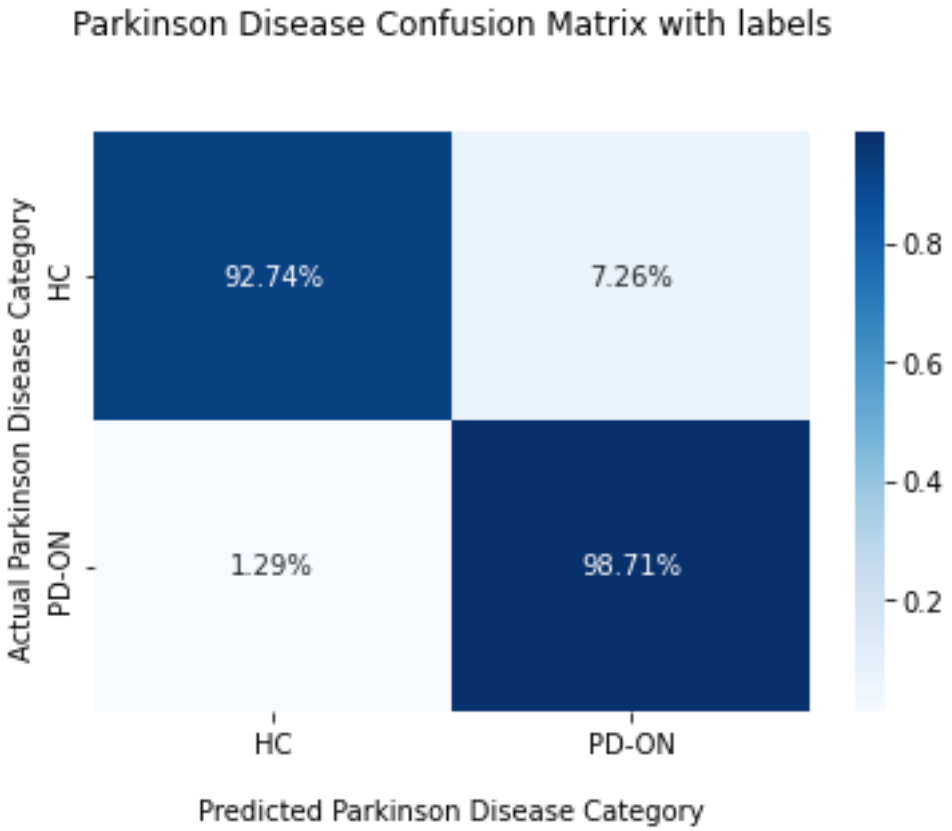

Figure 37: O1 channel HC and PD-ON Confusion Matrix

Accuracy = 0. 95625

Sensitivity = 0. 9870689655172413

Specificity = 0. 9274193548387096

The data of the O1 channel are divided into HC and PD-OFF. Then, it was trained and tested using AlexNet deep learning model and Google Colab. Obtained results are presented below.

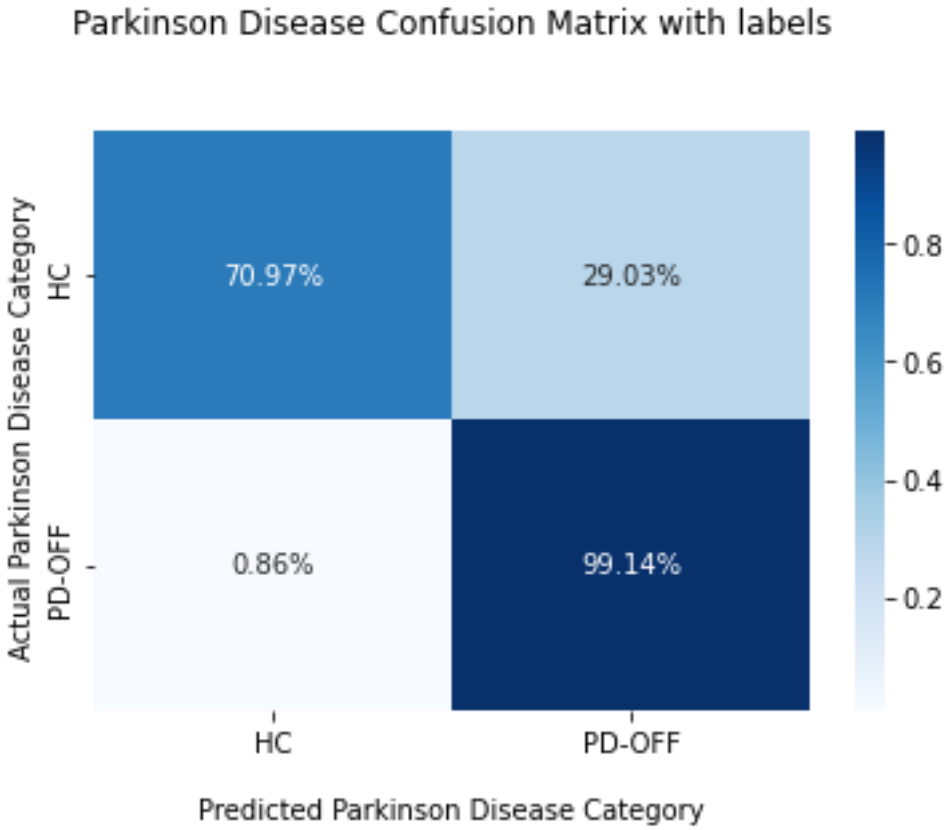

Figure 38: O1 channel HC and PD-OFF Confusion Matrix

Accuracy = 0. 8458333333333333

Sensitivity = 0. 9913793103448276

Specificity = 0. 7096774193548387

7.1.8 EEG Channel Oz

The data of the Oz channel are divided into HC and PD-ON. Then, it was trained and tested using AlexNet deep learning model and Google Colab. Obtained results are presented below.

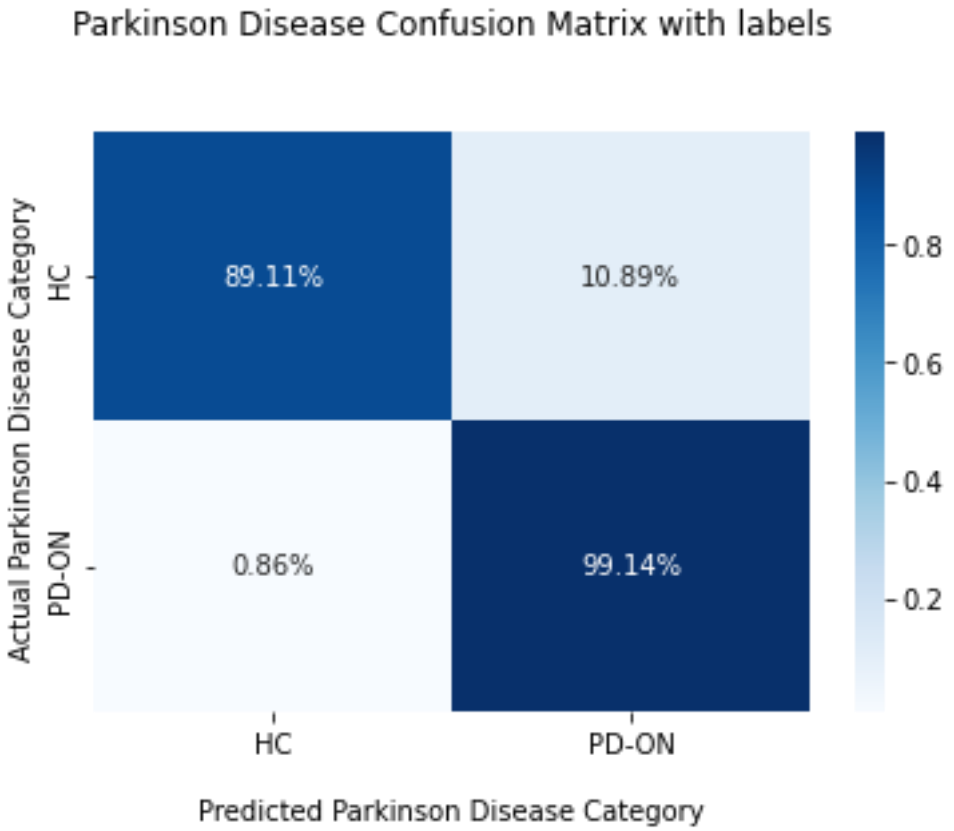

Figure 39: Oz channel HC and PD-ON Confusion Matrix

Accuracy = 0.9395833333333333

Sensitivity = 0.9913793103448276

Specificity = 0.8911290322580645

The data of the Oz channel are divided into HC and PD-OFF. Then, it was trained and tested using AlexNet deep learning model and Google Colab. Obtained results are presented below.

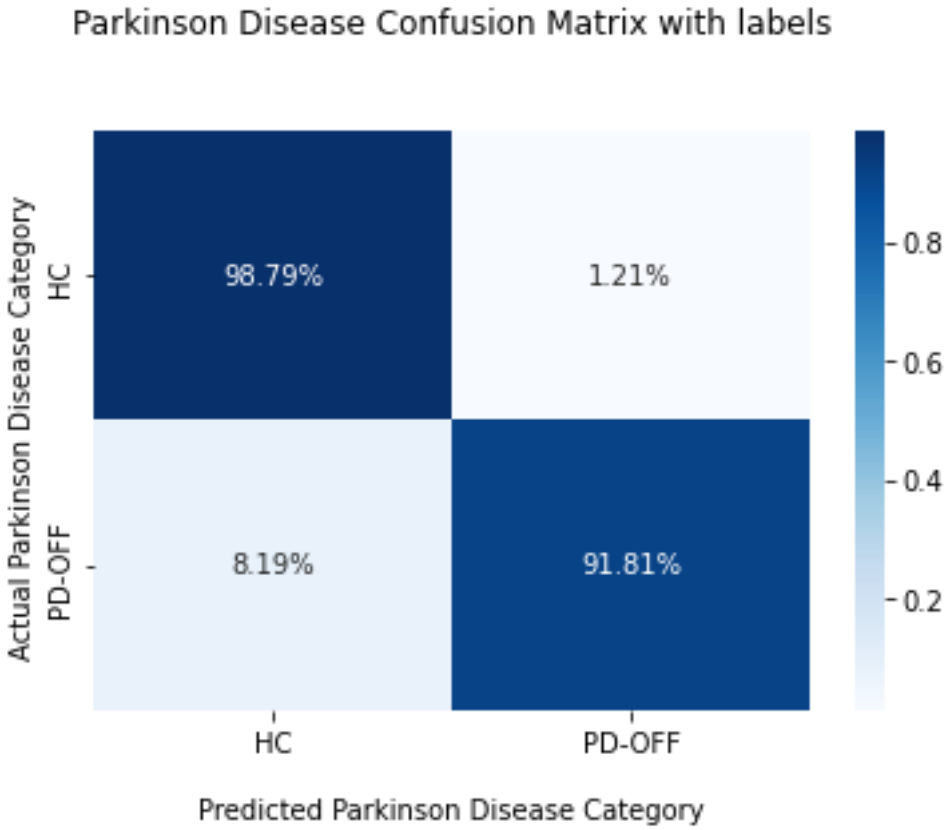

Figure 40: Oz channel HC and PD-OFF Confusion Matrix

Accuracy = 0. 9541666666666667

Sensitivity = 0. 9181034482758621

Specificity = 0. 9879032258064516

7.1.9 EEG Channel O2

The data of the O2 channel are divided into HC and PD-ON. Then, it was trained and tested using AlexNet deep learning model and Google Colab. Obtained results are presented below.

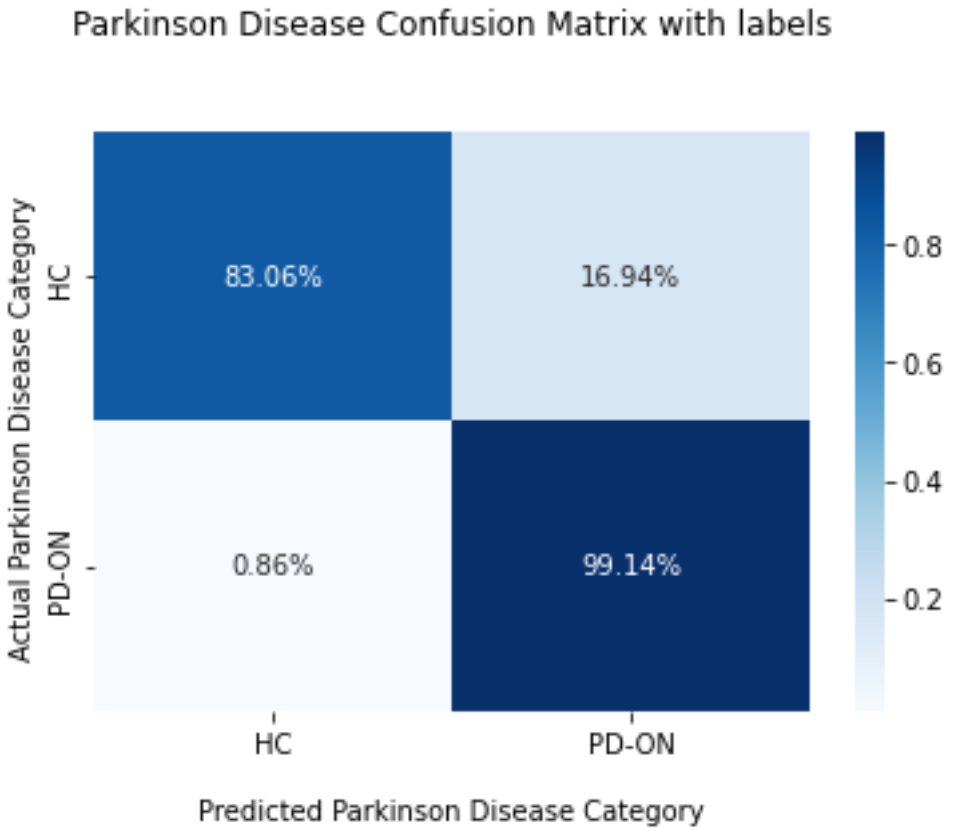

Figure 41: O2 channel HC and PD-ON Confusion Matrix

Accuracy = 0. 9083333333333333

Sensitivity = 0. 9913793103448276

Specificity = 0. 8306451612903226

The data of the O2 channel are divided into HC and PD-OFF. Then, it was trained and tested using AlexNet deep learning model and Google Colab. Obtained results are presented below.

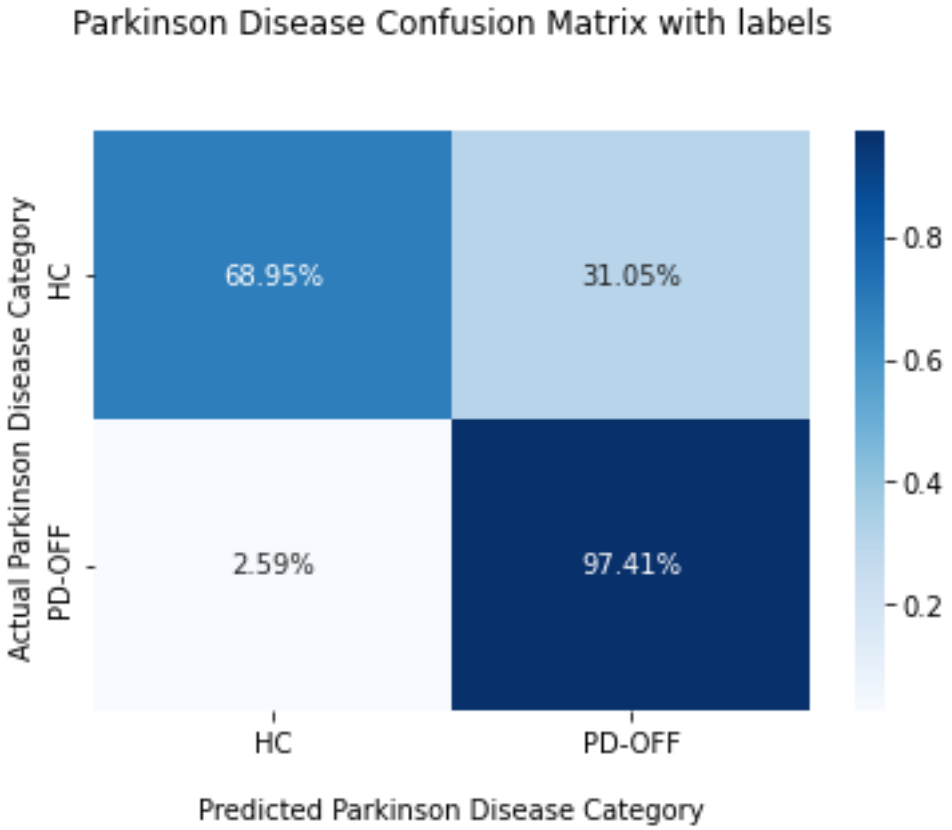

Figure 42: O2 channel HC and PD-OFF Confusion Matrix

Accuracy = 0. 8270833333333333

Sensitivity = 0. 9741379310344828

Specificity = 0. 6895161290322581

7.1.10 EEG Channel P4

The data of the P4 channel are divided into HC and PD-ON. Then, it was trained and tested using AlexNet deep learning model and Google Colab. Obtained results are presented below.

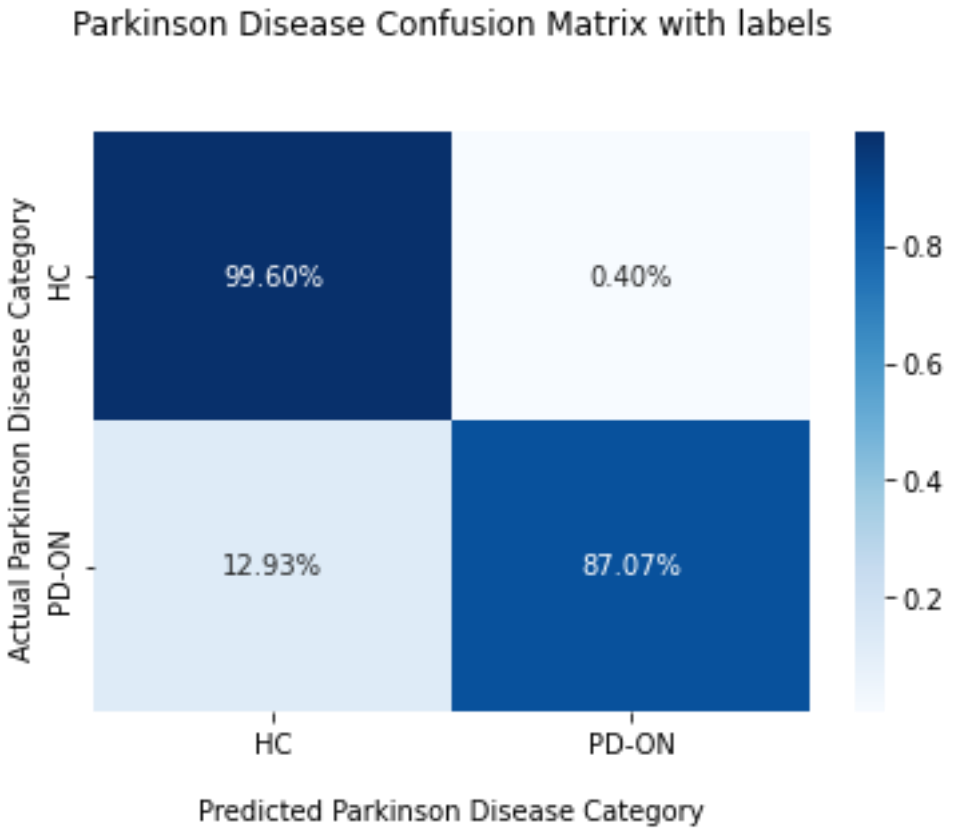

Figure 43: P4 channel HC and PD-ON Confusion Matrix

Accuracy = 0. 9354166666666667

Sensitivity = 0. 8706896551724138

Specificity = 0. 9959677419354839

The data of the P4 channel are divided into HC and PD-OFF. Then, it was trained and tested using AlexNet deep learning model and Google Colab. Obtained results are presented below.

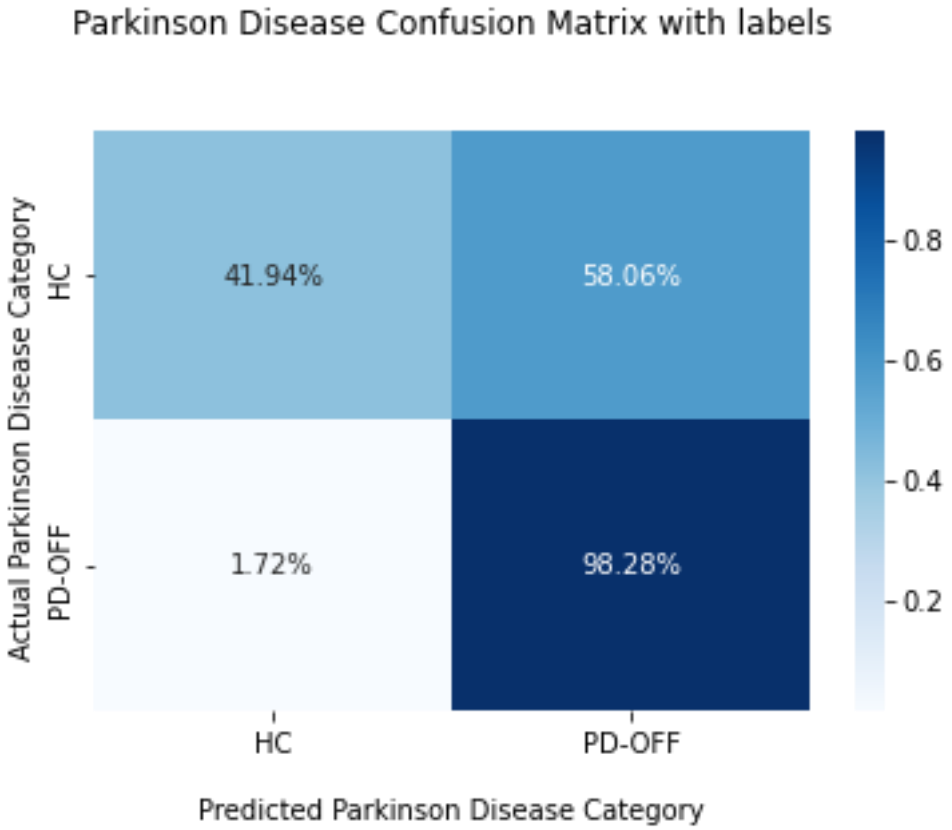

Figure 44: P4 channel HC and PD-OFF Confusion Matrix

Accuracy = 0. 6916666666666667

Sensitivity = 0. 9827586206896551

Specificity = 0. 41935483870967744

7.1.11 EEG Channel C4

The data of the C4 channel are divided into HC and PD-ON. Then, it was trained and tested using AlexNet deep learning model and Google Colab. Obtained results are presented below.

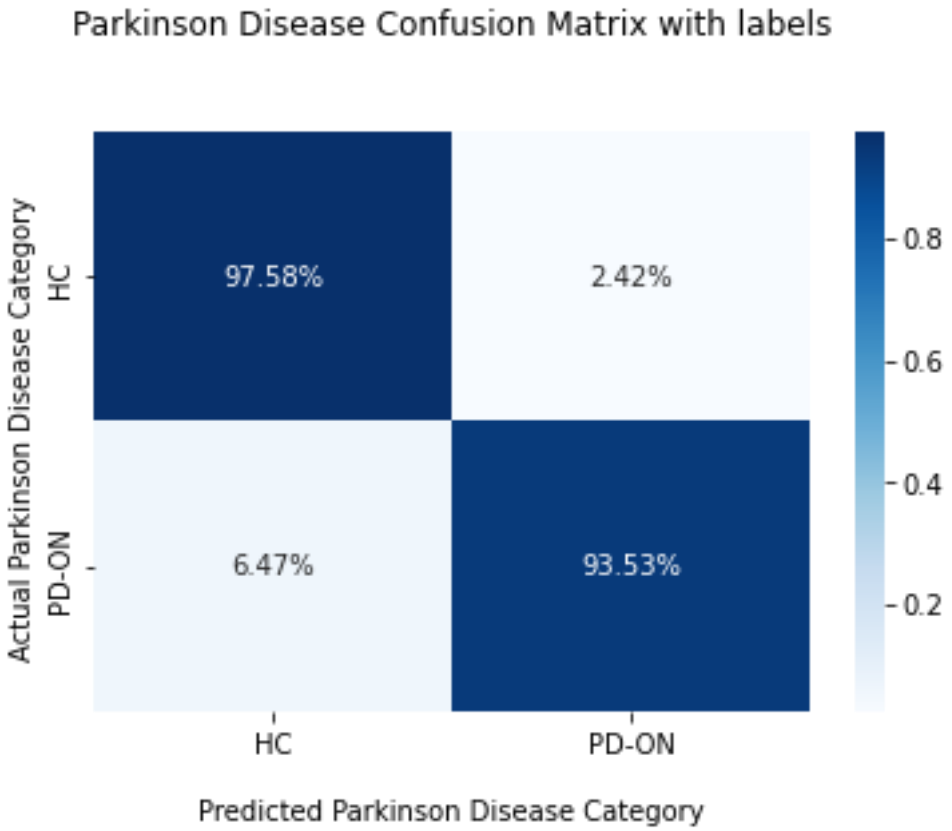

Figure 45: C4 channel HC and PD-ON Confusion Matrix

Accuracy = 0. 95625

Sensitivity = 0. 9353448275862069

Specificity = 0. 9758064516129032

The data of the C4 channel are divided into HC and PD-OFF. Then, it was trained and tested using AlexNet deep learning model and Google Colab. Obtained results are presented below.

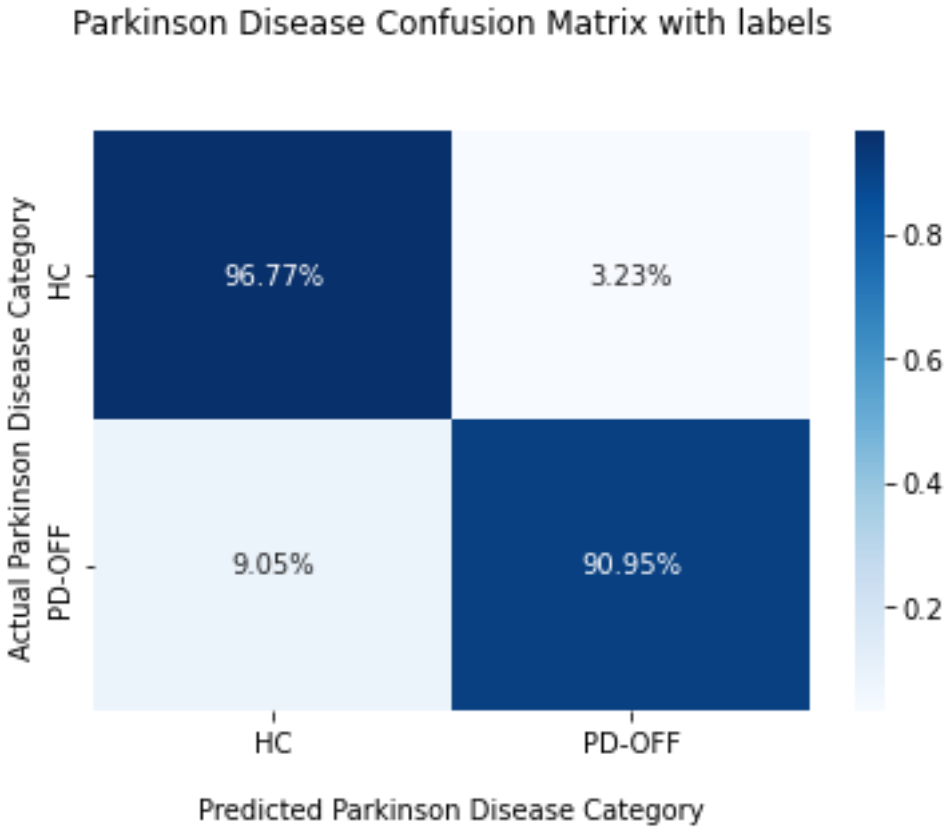

Figure 46: C4 channel HC and PD-OFF Confusion Matrix

Accuracy = 0. 9395833333333333

Sensitivity = 0. 9094827586206896

Specificity = 0. 967741935483871

7.1.12 EEG Channel F4

The data of the F4 channel are divided into HC and PD-ON. Then, it was trained and tested using AlexNet deep learning model and Google Colab. Obtained results are presented below.

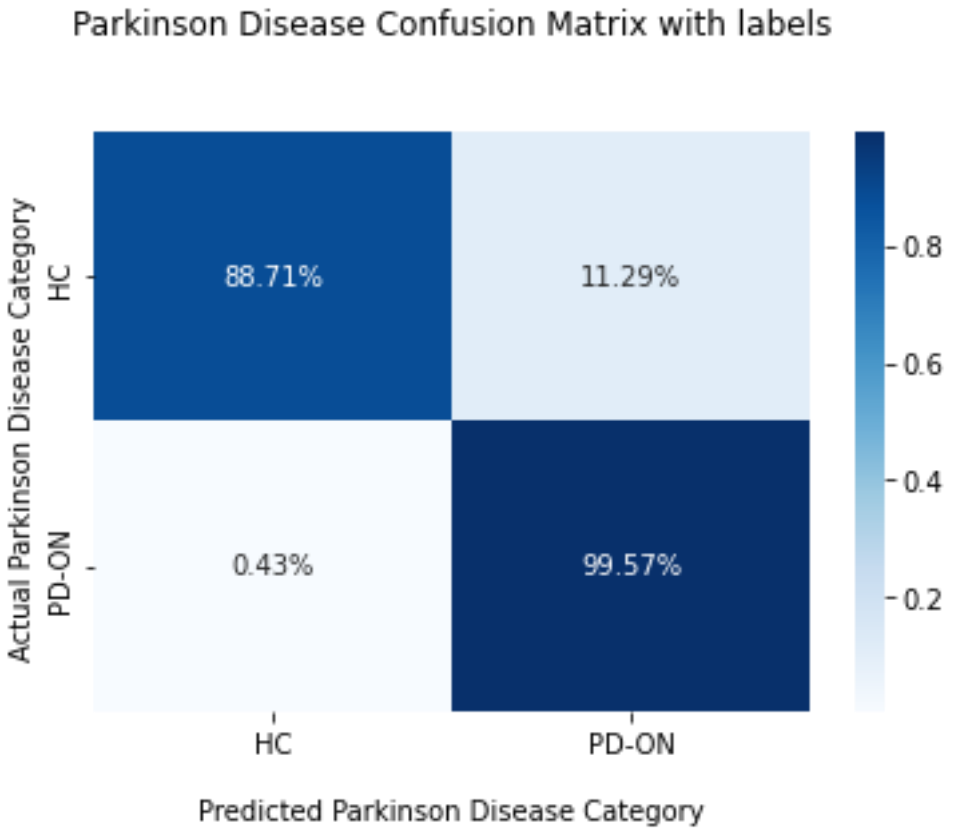

Figure 47: F4 channel HC and PD-ON Confusion Matrix

Accuracy = 0. 9395833333333333

Sensitivity = 0. 9956896551724138

Specificity = 0. 8870967741935484

The data of the F4 channel are divided into HC and PD-OFF. Then, it was trained and tested using AlexNet deep learning model and Google Colab. Obtained results are presented below.

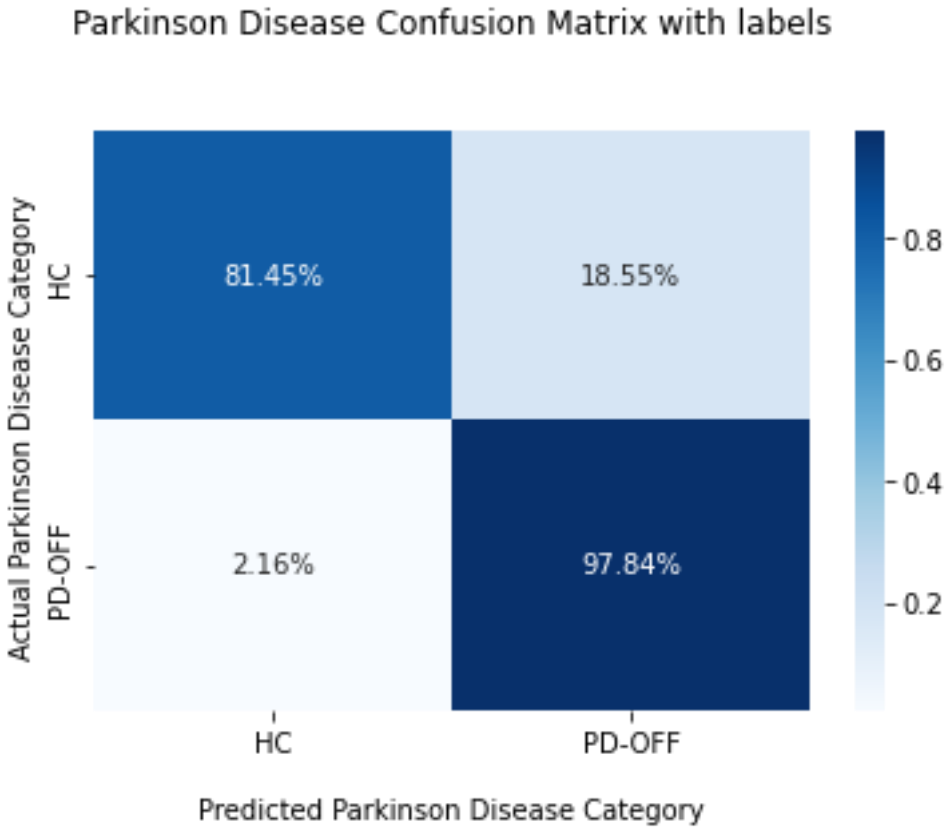

Figure 48: F4 channel HC and PD-OFF Confusion Matrix

Accuracy = 0. 89375

Sensitivity = 0. 978448275862069

Specificity = 0. 8145161290322581

7.1.13 EEG Channel F8

The data of the F8 channel are divided into HC and PD-ON. Then, it was trained and tested using AlexNet deep learning model and Google Colab. Obtained results are presented below.

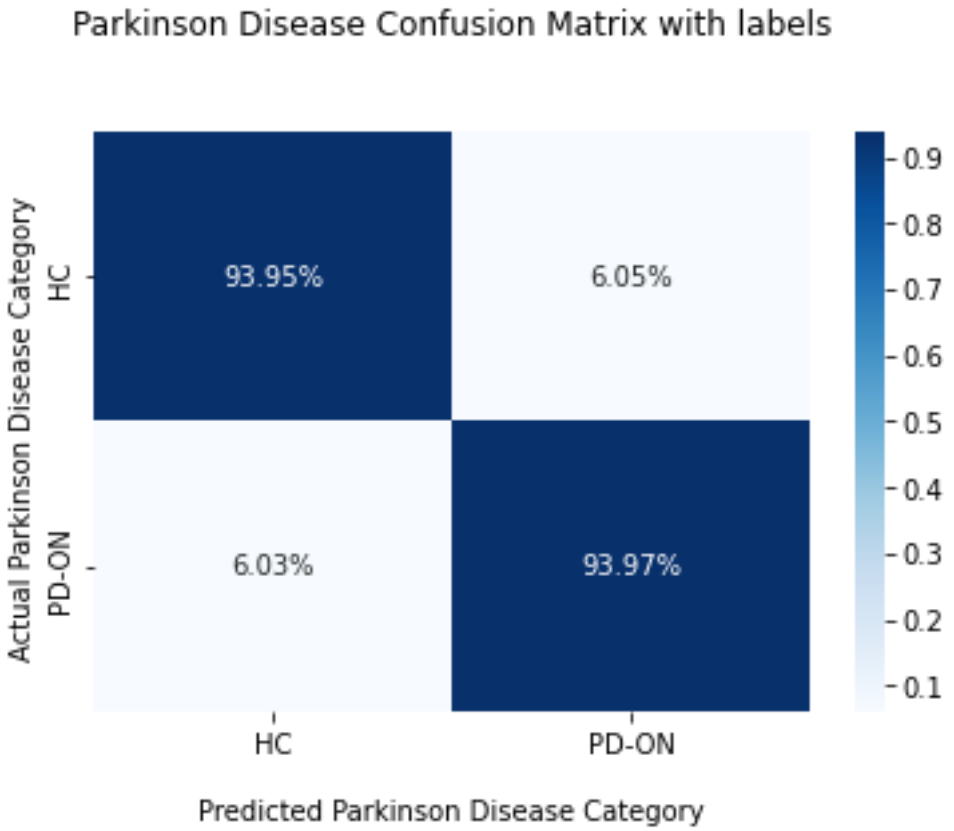

Figure 49: F8 channel HC and PD-ON Confusion Matrix

Accuracy = 0. 9395833333333333

Sensitivity = 0. 9396551724137931

Specificity = 0. 9395161290322581

The data of the F8 channel are divided into HC and PD-OFF. Then, it was trained and tested using AlexNet deep learning model and Google Colab. Obtained results are presented below.

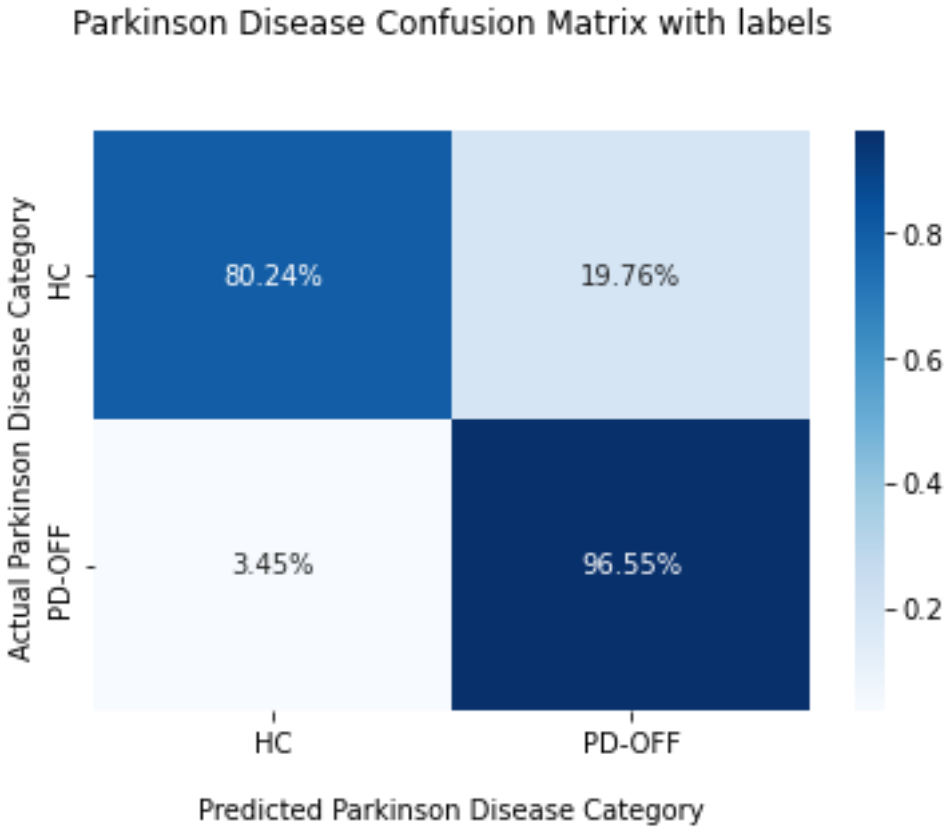

Figure 50: F8 channel HC and PD-OFF Confusion Matrix

Accuracy = 0. 88125

Sensitivity = 0. 9655172413793104

Specificity = 0. 8024193548387096

7.1.14 EEG Channel Fp2

The data of the Fp2 channel are divided into HC and PD-ON. Then, it was trained and tested using AlexNet deep learning model and Google Colab. Obtained results are presented below.

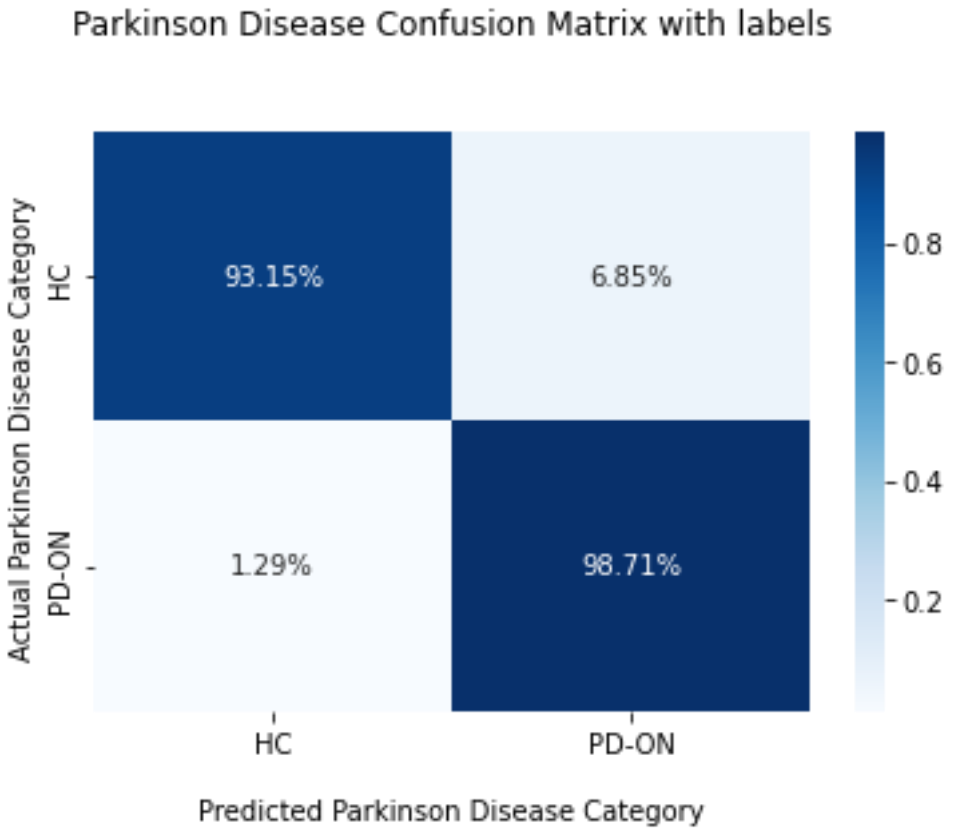

Figure 51: Fp2 channel HC and PD-ON Confusion Matrix

Accuracy = 0. 9583333333333334

Sensitivity = 0. 9870689655172413

Specificity = 0. 9314516129032258

The data of the Fp2 channel are divided into HC and PD-OFF. Then, it was trained and tested using AlexNet deep learning model and Google Colab. Obtained results are presented below.

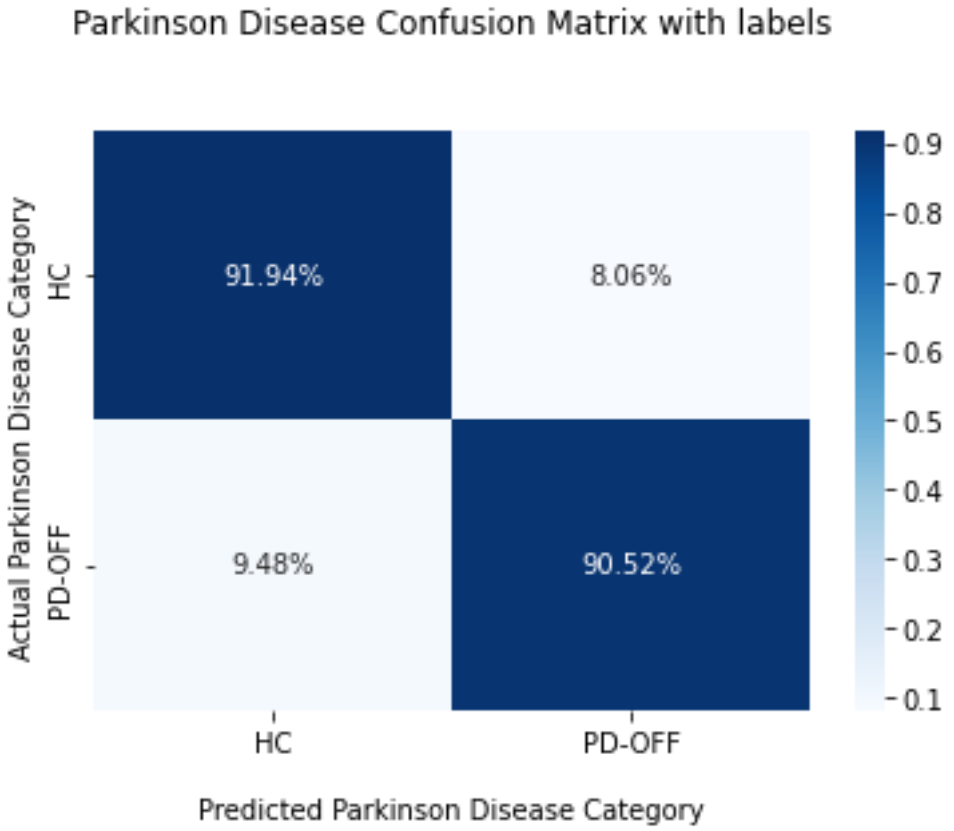

Figure 52: Fp2 channel HC and PD-OFF Confusion Matrix

Accuracy = 0. 9125

Sensitivity = 0. 9051724137931034

Specificity = 0. 9193548387096774

7.1.15 EEG Channel Fz

The data of the Fz channel are divided into HC and PD-ON. Then, it was trained and tested using AlexNet deep learning model and Google Colab. Obtained results are presented below.

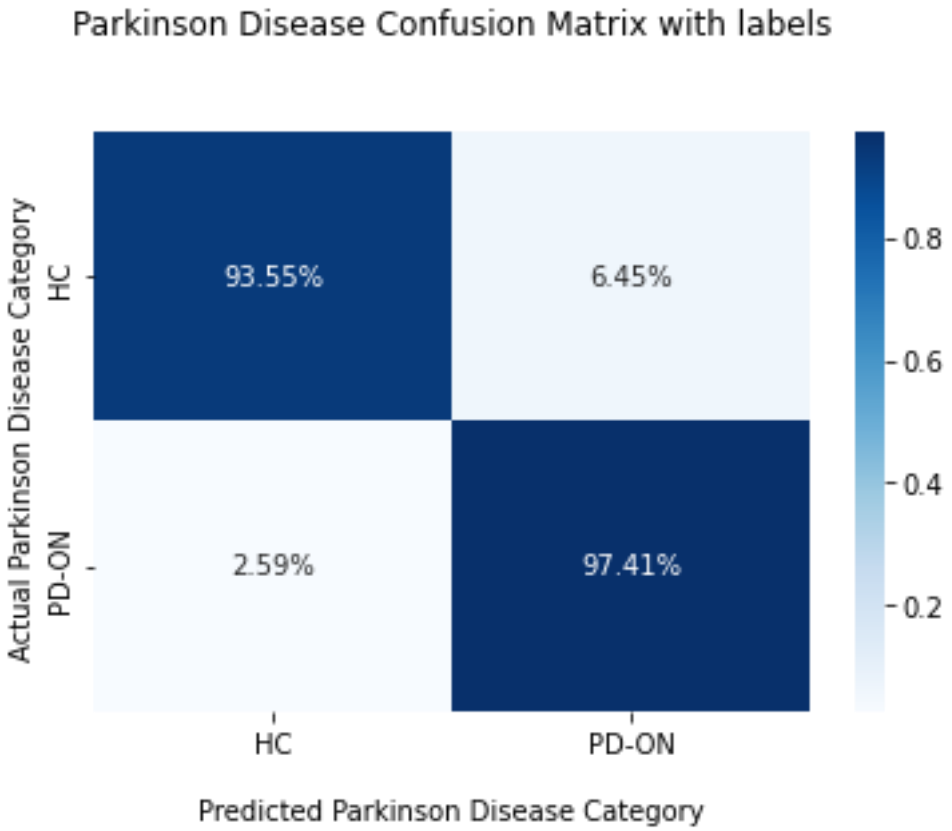

Figure 53: Fz channel HC and PD-ON Confusion Matrix

Accuracy = 0. 9541666666666667

Sensitivity = 0. 9741379310344828

Specificity = 0. 9354838709677419

The data of the Fz channel are divided into HC and PD-OFF. Then, it was trained and tested using AlexNet deep learning model and Google Colab. Obtained results are presented below.

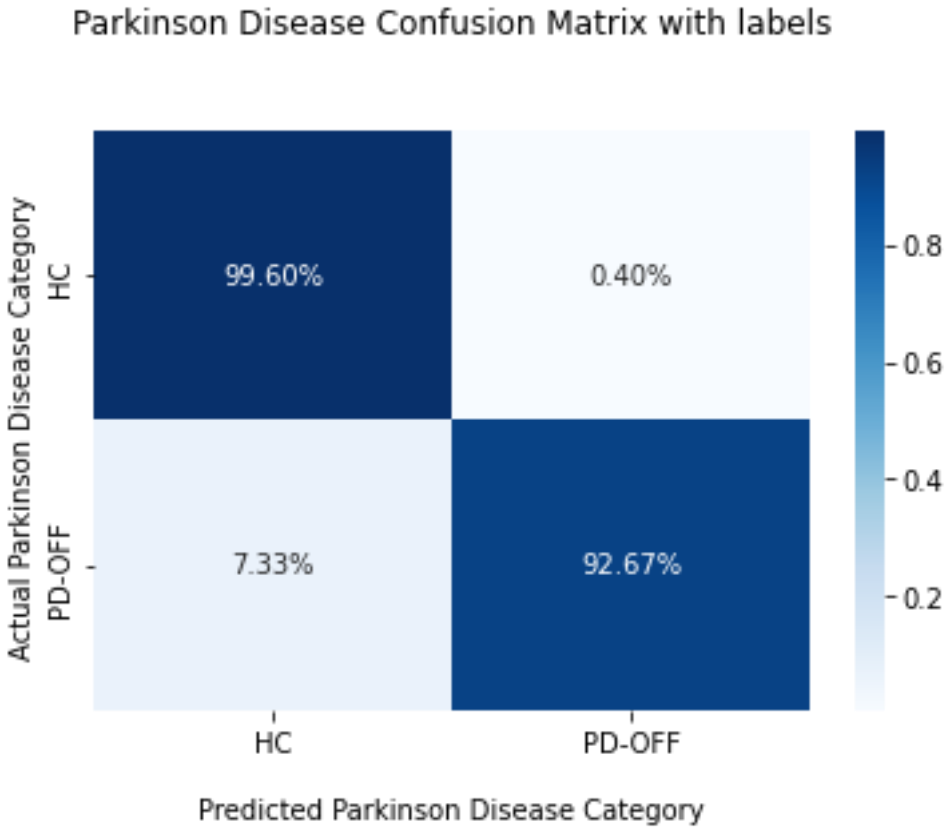

Figure 54: Fz channel HC and PD-OFF Confusion Matrix

Accuracy = 0. 9625

Sensitivity = 0. 9267241379310345

Specificity = 0. 9959677419354839

7.1.16 EEG Channel Cz

The data of the Cz channel are divided into HC and PD-ON. Then, it was trained and tested using AlexNet deep learning model and Google Colab. Obtained results are presented below.

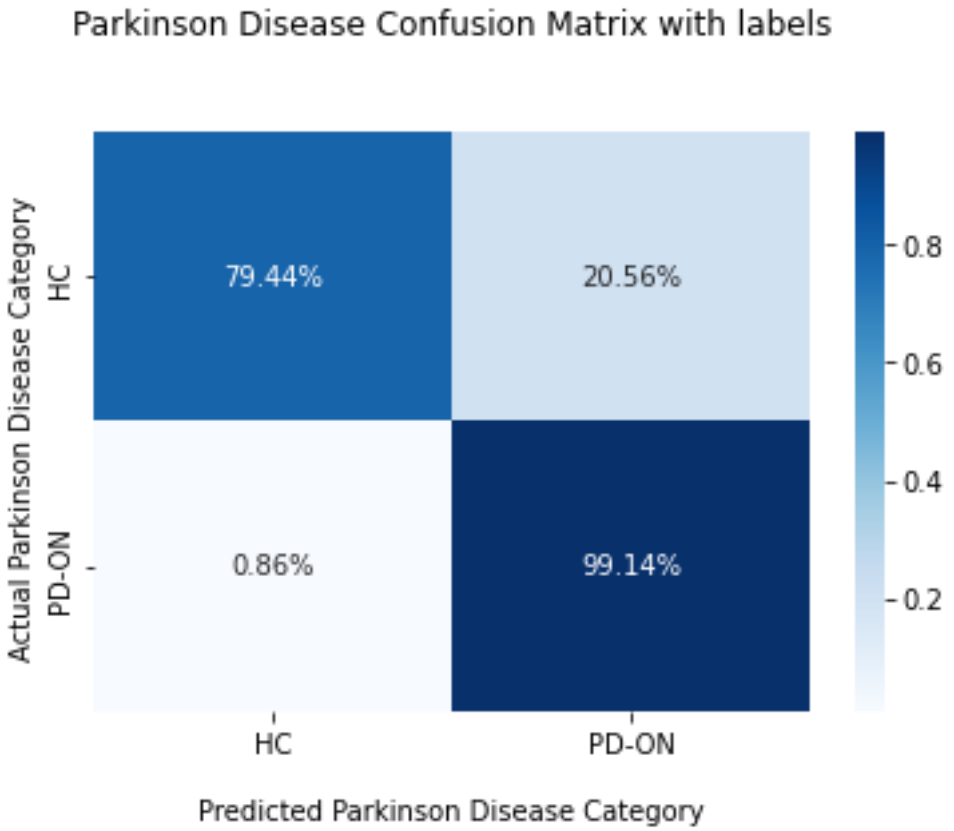

Figure 55: Cz channel HC and PD-ON Confusion Matrix

Accuracy = 0. 8895833333333333

Sensitivity = 0. 9913793103448276

Specificity = 0. 7943548387096774

The data of the Cz channel are divided into HC and PD-OFF. Then, it was trained and tested using AlexNet deep learning model and Google Colab. Obtained results are presented below.

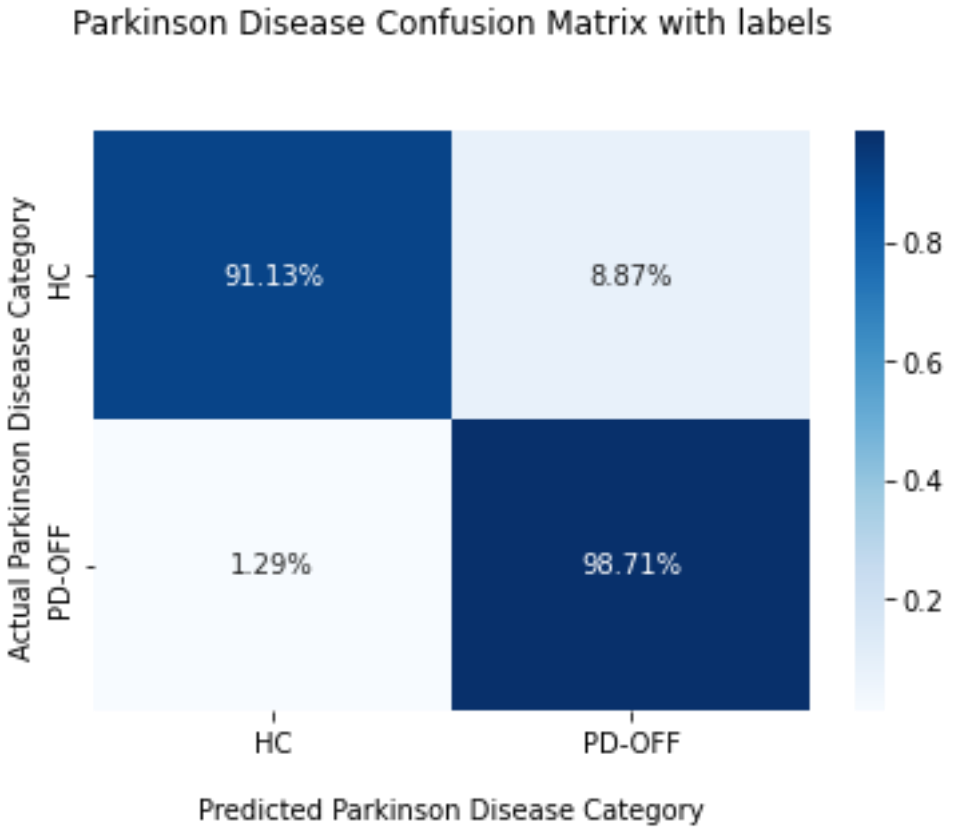

Figure 56: Cz channel HC and PD-OFF Confusion Matrix

Accuracy = 0. 9479166666666666

Sensitivity = 0. 9870689655172413

Specificity = 0. 9112903225806451

7.2 General Results

All channels are individually trained and tested using Google Colab. Obtained results are presented below.

Table 2: Results of all channels

Channel	PD-ON			PD-OFF		
	Accuracy	**Sensitivity**	**Specificity**	**Accuracy**	**Sensitivity**	**Specificity**
Fp1	0.97	0.97	0.96	0.98	0.98	0.99
F7	0.96	0.97	0.95	0.98	0.98	0.99
F3	0.98	0.99	0.98	0.96	0.96	0.96
C3	0.81	0.99	0.65	0.95	0.94	0.97
P3	0.90	0.99	0.83	0.75	0.99	0.52
Pz	0.95	0.98	0.93	0.92	0.99	0.87
O1	0.95	0.98	0.92	0.84	0.99	0.70
Oz	0.93	0.99	0.89	0.95	0.91	0.98
O2	0.90	0.99	0.83	0.82	0.97	0.68
P4	0.93	0.87	0.99	0.69	0.98	0.41
C4	0.95	0.93	0.97	0.93	0.90	0.96
F4	0.93	0.99	0.88	0.89	0.97	0.81
F8	0.93	0.93	0.93	0.8	0.96	0.80
Fp2	0.95	0.98	0.93	0.91	0.90	0.91
Fz	0.95	0.97	0.93	0.96	0.92	0.99
Cz	0.88	0.99	0.79	0.94	0.98	0.91

All channels have been individually trained and tested using Google Colab. It has been observed that a maximum of 3 channels can be operated simultaneously with the GPU memory of Google colab. For this reason, it was desired to train and test by selecting the 3 channels with the highest results. In the results obtained, it was observed that the highest results were obtained in the Fc1, F7 and F3 channels. For this reason, the data of these 3 channels were combined into a single file.

A single HC file was obtained by combining the HC files of 3 channels. This is also done for PD-ON and PD-OFF. GPU memory is insufficient when k-fold Cross Validation is used to get better results while running the model. In order to apply K-fold Cross Validation, 20000 images were randomly selected from each file (HC, PD-ON, PD-OFF) in order to minimize the data in the selected 3 channels. The resulting file contains a total of 60000 images. It allows 60000 visuals to work without exceeding the memory capacity of the system.

The results are presented in 2 different ways. The first of these was obtained using only PD-ON and HC. The latter was obtained using HC and PD-OFF.

All of the same processes were trained and tested in k-fold Cross Validation. All results are listed below.

F7, F3, Fp1 channels data for HC and PD-OFF. It was trained and tested using the AlexNet deep learning model and Google Colab. Obtained results are presented below.

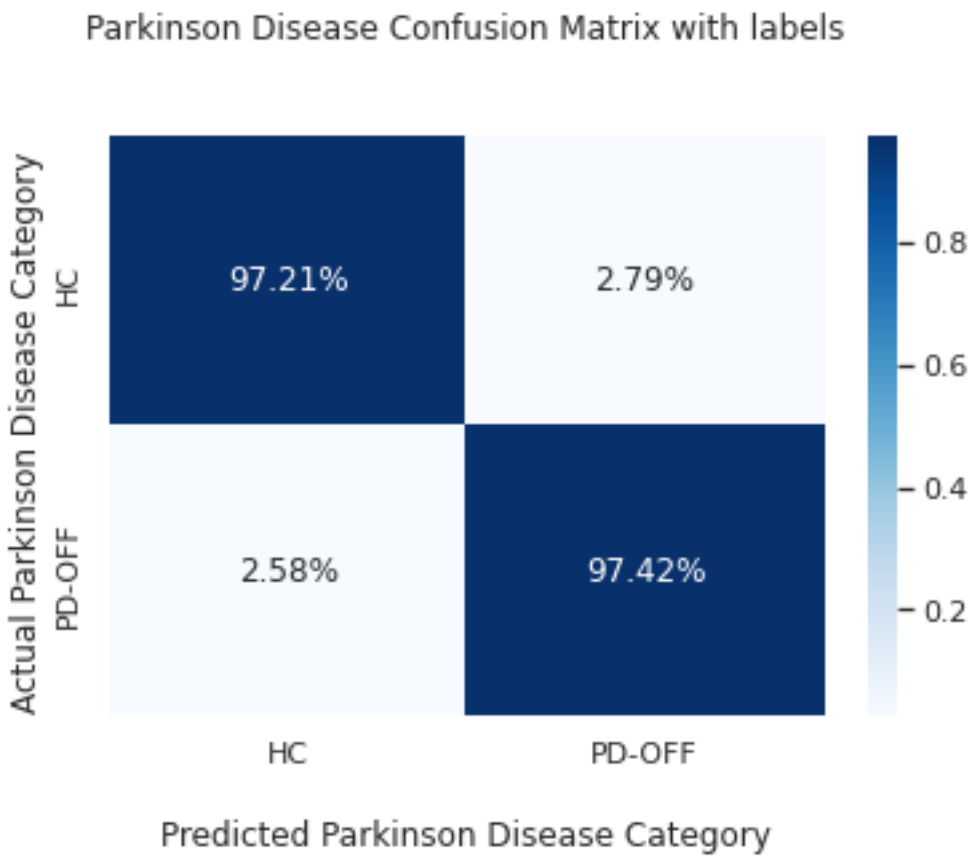

Figure 57: Fp1, F7, F3 channel HC and PD-OFF Confusion Matrix

Accuracy = 0.9732

Sensitivity = 0.9742472266244057

Specificity = 0.9721324717285945

F7, F3, Fp1 channels data for HC and PD-ON. It was trained and tested using the AlexNet deep learning model and Google Colab. Obtained results are presented below.

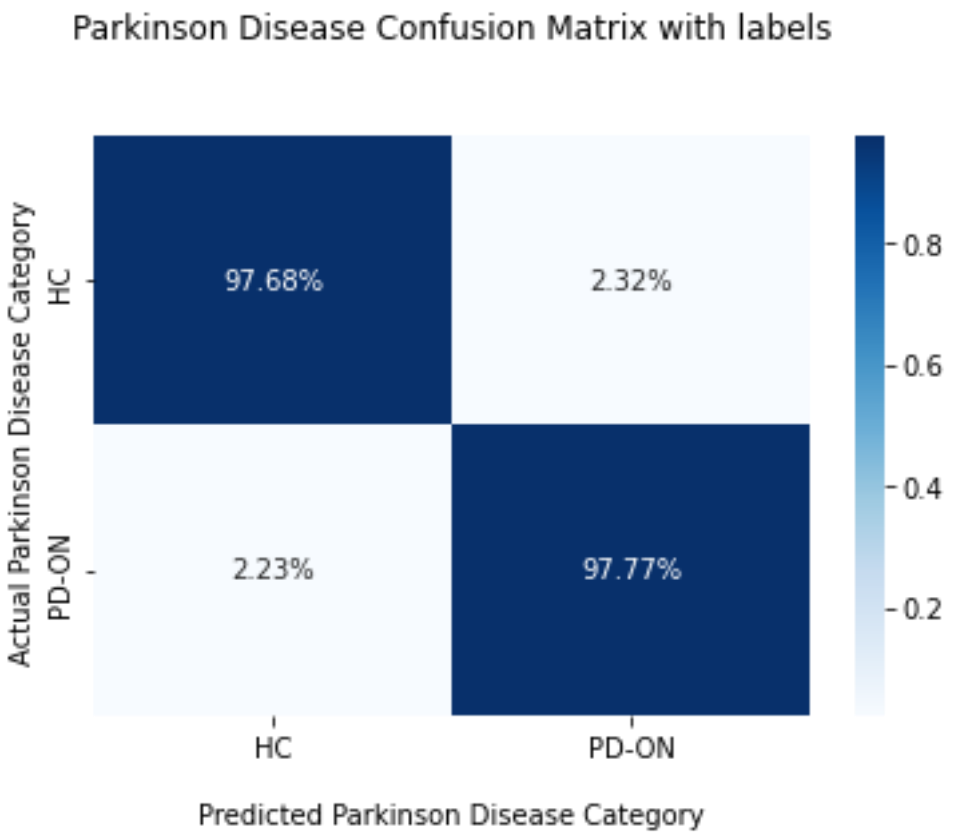

Figure 58: Fp1, F7, F3 channel HC and PD-ON Confusion Matrix

Accuracy = 0. 97725

Sensitivity = 0. 9776876267748479

Specificity = 0. 9768244575936884

7.2.1 General Results With K-Fold

K-Fold Cross Validation was used to get better results.[15] Google Colab's gpu capacity is suitable for 4-Fold at most. Therefore, the model was trained and tested along 4-Fold using K-Fold Cross Validation. This was done using the F7, F3, Fp1 channel data for HC and PD-OFF. Obtained results are presented below.

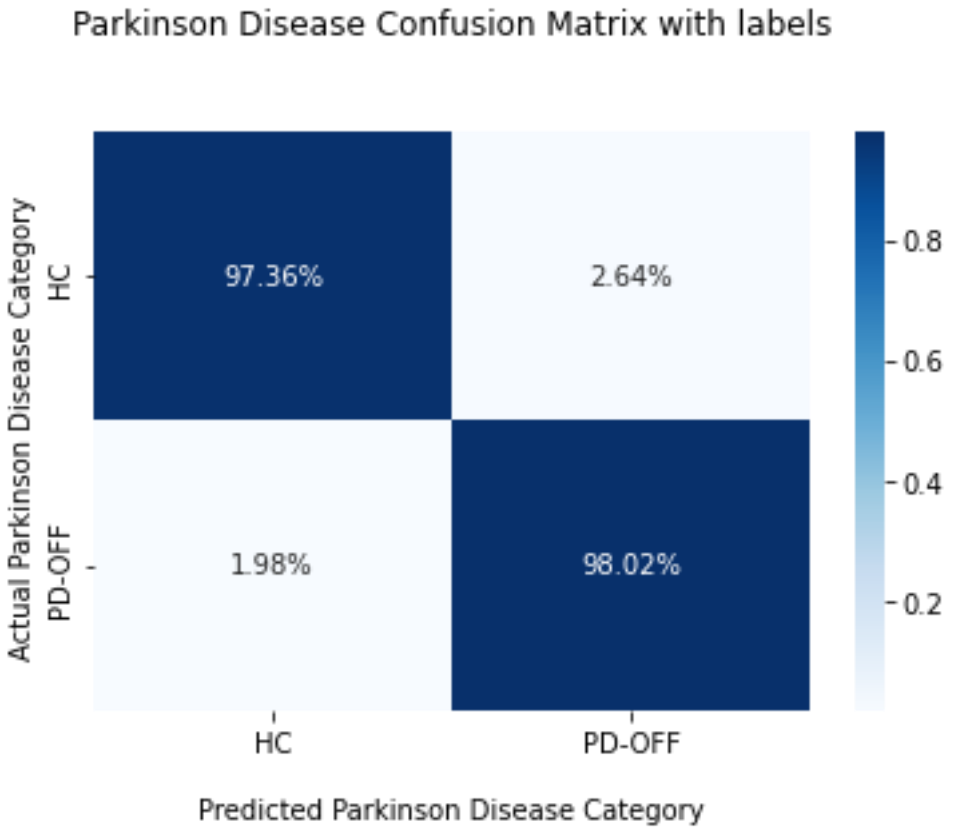

Figure 59: Fp1, F7, F3 channel HC and PD-OFF Confusion Matrix

Accuracy = 0. 976875

Sensitivity = 0. 9802080690180157

Specificity = 0. 9736388272973638

K-Fold Cross Validation was used to get better results.[15] In addition, the model was trained and tested along 4-Fold using K-Fold Cross Validation. This was done using the F7, F3, Fp1 channel data for HC and PD-ON. Obtained results are presented below.

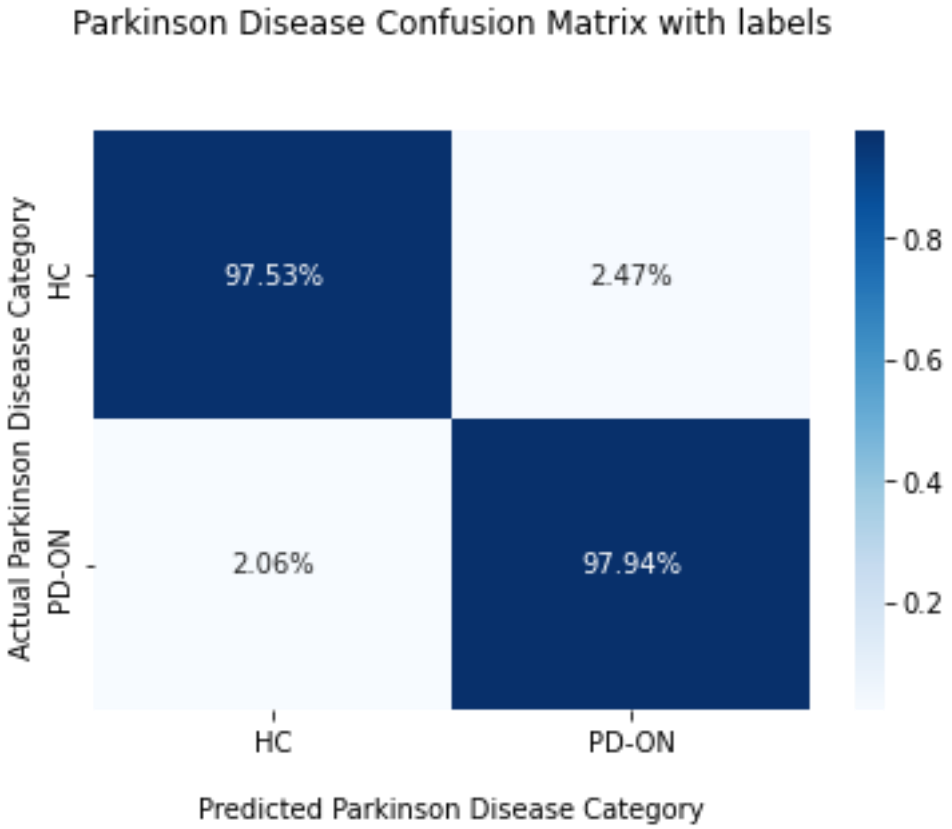

Figure 60: Fp1, F7, F3 channel HC and PD-ON Confusion Matrix

Accuracy = 0.977375

Sensitivity = 0.9794383149448345

Specificity = 0.9753240279162513

7.3 Discussion

All the results obtained were compared with similar studies conducted in recent years.

The following comparison table presents the dataset used and the selected channels.

Table 3:Another studies with dataset and channels

Authors	Channels	Dataset
Wang et al. [21]	14 channel	Private - From the Henan Provincial People's Hospital (People's Hospital of Zhengzhou University)
Ward et al. [22]	F3, O1, OZ, O2	Private - From the Neuroscan SynAmps2 acquisition system (Neuroscan, VA, United States)
Khare et al. [23]	C3	UC San Diego Resting State EEG Data 2019
Hagiwara et al. [2]	14 channel	Private - From the Hospital Universiti Kebangsaan Malaysia.
Palmer et al. [24]	32 channel	UC San Diego Resting State EEG Data 2020
Shaban et al. [3]	OZ, P8, FC2	UC San Diego Resting State EEG Data 2020
Cahoon et al. [5]	FP1 FC1, CP5, FZ	UC San Diego Resting State EEG Data 2021
Lee et al. [25]	27 channel	Private - From the Clinical Research at the University of British Columbia (UBC)
Amara et al. [26]	FP1, FP2, CP5, FC1	UC San Diego Resting State EEG Data - 2021
This work	FP1, F7, F3	UC San Diego Resting State EEG Data - 2022
This work with K-Fold	FP1, F7, F3	UC San Diego Resting State EEG Data - 2022

In the studies presented in the table above, the neural network used and the results obtained are presented in the table below.

Table 4: Results and other studies

Authors	Year	Techniques	Accuracy	Sensitivity	Specificity
Wang et al. [21]	2020	RNN	88.31	84.84	91.81
Ward et al. [22]	2021	RNN	99.2	98.9	99.4
Khare et al. [23]	2021	LSSVM	96.13	97.65	97.0
Hagiwara et al. [2]	2020	CNN	88.25	84.71	91.77
Palmer et al. [24]	2021	CNN	99.46	x	x
Shaban et al. [3]	2021	ANN	98	97	100
Cahoon et al. [5]	2021	CNN	99.9	x	x
Lee et al. [25]	2019	CNN	96.9	100	93.4
Amara et al. [26]	2022	CNN	99.9	99.6	99.8
This work	2022	CNN	97.72	97.76	97.68
This work with K-Fold	2022	CNN	97.73	97.94	97.53

In this study, two different results were obtained. With a slight difference between the results obtained, the 4-fold model gave higher results. There are many studies using different techniques and different neural networks in the early diagnosis of Parkinson's disease. Although CNN was used in the majority of these studies, ANN, LSSVM and RNN neural network models were also used, unlike CNN. In the table above, the studies conducted in this field and the results of these studies are presented. The GASF technique we used and the deep CNN model gave a very high result with 97.73. When compared with other studies in this field, it was observed that the GASF technique and CNN deep network used gave higher results than most of the other studies. However, it has been observed that there are more successful studies in this field.

Chapter 8

CONCLUSION

There is no treatment for Parkinson's disease. However, the progression of Parkinson's disease can be slowed down with drug treatment. Parkinson's disease consists of 5 phases. For a patient who has reached the fifth stage, a medication is no longer possible. Therefore, it is very important to diagnose Parkinson's disease before its stages progress and to start drug treatment in order to slow down the progression of the disease. Parkinson's disease can only be diagnosed by a neurologist. In this study, it is aimed to diagnosis early stages of Parkinson's disease with artificial intelligence.

As a result, in this study, it is aimed to classify 2D images with AlexNet CNN model by using GASF technique for early diagnosis of Parkinson's disease. The results obtained are promising. Although the success of the CNN model was proven in 2D images, it was not known how successful it was in classifying GASF images. This study has proven that the GASF technique is at least as successful as the techniques in other studies.

When the results were examined, satisfactory results were obtained with the AlexNet CNN model with 97.73% Accuracy, 97.94% Sensitivity and 97.53% Specificity.

Chapter 9

IN THE FUTURE

In this study, the deep learning model was trained and tested by creating 2D images with the Gramian Angular Summation Field (GASF) technique. In the future, it is predicted that Gramian Angular Difference Field (GADF) and Markov Transition Fields (MTF) techniques such as GASF can be used to obtain higher results than these obtained results.

In addition, even if the success of the CNN model has been proven in the classification of 2D dimensional images, it has been observed that higher results can be obtained with RNN in some studies in the literature. It is predicted that high results can be obtained by using RNN neural network instead of CNN in the future.

REFERENCES

[1] Pernet, C. R., Appelhoff, S., Gorgolewski, K. J., Flandin, G., Phillips, C., Delorme, A., & Oostenveld, R. (2019). EEG-BIDS, an extension to the brain imaging data structure for electroencephalography. *Scientific data,* 6(1), 1-5.

[2] Oh, S. L., Hagiwara, Y., Raghavendra, U., Yuvaraj, R., Arunkumar, N., Murugappan, M., & Acharya, U. R. (2020). A deep learning approach for Parkinson's disease diagnosis from EEG signals. *Neural Computing and Applications,* 32(15), 10927-10933.

[3] Shaban, M. (2021, May). Automated screening of parkinson's disease using deep learning based electroencephalography. *In 2021 10th International IEEE/EMBS Conference on Neural Engineering (NER)* (pp. 158-161). IEEE.

[4] Vanegas, M. I., Ghilardi, M. F., Kelly, S. P., & Blangero, A. (2018, December). Machine learning for EEG-based biomarkers in Parkinson's disease. *In 2018 IEEE International Conference on Bioinformatics and Biomedicine (BIBM)* (pp. 2661-2665). IEEE.

[5] Cahoon, S., Khan, F., Polk, M., & Shaban, M. (2021, December). Wavelet-based convolutional neural network for parkinson's disease detection in resting-state electroencephalography. *In 2021 IEEE Signal Processing in Medicine and Biology Symposium (SPMB)* (pp. 1-5). IEEE.

[6] Bragin, A. D., & Spitsyn, V. G. (2019). Electroencephalogram analysis based on gramian angular fieldtransformation. *In CEUR Workshop Proceedings* (Vol. 24852019, pp. 273-275).

[7] Lacko, D. (2017). The application of 3D anthropometry for the development of headgear-a case study on the design of ergonomic brain-computer interfaces.

[8] Wikimedia Foundation. (2022, March 13). 10 20 system (EEG). Wikipedia. Retrieved July 20, 2022, from https://en.wikipedia.org/wiki/10%E2%80%9320_system_%28EEG%29

[9] Ramakrishnan, A. G., & Satyanarayana, J. V. (2016). Reconstruction of EEG from limited channel acquisition using estimated signal correlation. *Biomedical Signal Processing and Control*, 27, 164 173.

[10] Krizhevsky, A., Sutskever, I., & Hinton, G. E. (2012). Imagenet classification with deep convolutional neural networks. *Advances in neural information processing systems*, 25.

[11] Han, X., Zhong, Y., Cao, L., & Zhang, L. (2017). Pre-trained alexnet architecture with pyramid pooling and supervision for high spatial resolution remote sensing image scene classification. *Remote Sensing*, 9(8), 848.

[12] LeCun, Y., Bottou, L., Bengio, Y., & Haffner, P. (1998). Gradient-based learning applied to document recognition. *Proceedings of the IEEE,* 86(11), 2278-2324.

[13] Feng, J., He, X., Teng, Q., Ren, C., Chen, H., & Li, Y. (2019). Reconstruction of porous media from extremely limited information using conditional generative adversarial networks. *Physical Review E*, *100*(3), 033308.

[14] Wang, Z., & Oates, T. (2015, June). Imaging time-series to improve classification and imputation. *In Twenty Fourth International Joint Conference on Artificial Intelligence.*

[15] Refaeilzadeh, P., Tang, L., & Liu, H. (2009*). Cross-validation. Encyclopedia of database systems*, 5, 532-538.

[16] Alexander P. Rockhill and Nicko Jackson and Jobi George and Adam Aron and Nicole C. Swann (2021). UC San Diego Resting State EEG Data from Patients with Parkinson's disease _ OpenNeuro. [Dataset] doi: doi:10.18112/openneuro.ds002778.v 1.0.5

[17] Merlin Praveena, D., Angelin Sarah, D., & Thomas George, S. (2020). Deep learning techniques for EEG signal applications a review. *IETE Journal of Research*, 1 8.

[18] Alnajjar, M. (2021). Image-Based Detection Using Deep Learning and Google Colab.

[19] Hussain, S., Dixit, P., & Hussain, M. S. (2020). Image Processing in Artificial Intelligence.

[20] Marques, L., Lopes, L., Ferreira, M., Wanzeller, C., Martins, P., & Abbasi, M. (2022). Image Processing: Impact of Train and Test Sizes on Custom Image Recognition Algorithms. In *Marketing and Smart Technologies* (pp. 365-380). Springer, Singapore.

[21] Xu, S., Wang, Z., Sun, J., Zhang, Z., Wu, Z., Yang, T., ... & Cheng, C. (2020). Using a deep recurrent neural network with EEG signal to detect Parkinson's disease. *Annals of translational medicine,* 8(14).

[22] Lee, S., Hussein, R., Ward, R., Wang, Z. J., & McKeown, M. J. (2021). A convolutional recurrent neural network approach to resting state EEG classification in Parkinson's disease. *Journal of neuroscience methods*, 361, 109282.

[23] Khare, S. K., Bajaj, V., & Acharya, U. R. (2021). Detection of Parkinson's disease using automated tunable Q wavelet transform technique with EEG signals. *Biocybernetics and Biomedical Engineering*, 41(2), 679-689.

[24] Loh, H. W., Ooi, C. P., Palmer, E., Barua, P. D., Dogan, S., Tuncer, T., ... & Acharya, U. R. (2021). GaborPDNet: Gabor transformation and deep neural network for Parkinson's disease detection using EEG signals. *Electronics*, 10(14), 1740.

[25] Lee, S., Hussein, R., & McKeown, M. J. (2019, November). A deep convolutional-recurrent neural network architecture for Parkinson's disease EEG classification. In *2019 IEEE Global Conference on Signal and Information Processing (GlobalSIP)* (pp. 1-4). IEEE.

[26] Shaban, M., & Amara, A. W. (2022). Resting state electroencephalography based deep-learning for the detection of Parkinson's disease. *Plos one,* 17(2), e0263159.